

Highlights

Port-Hamiltonian formulations for the modeling, simulation and control of fluids

Flávio Luiz Cardoso-Ribeiro, Ghislain Haine, Yann Le Gorrec, Denis Matignon, Hector Ramirez

- A comprehensive review of the port-Hamiltonian framework applied to fluid problems.
- A modular approach to the physical modeling of fluids as open systems, including conservative or dissipative phenomena.
- A structure-preserving numerical method for which the continuous power balance carries over to the discrete level.
- Input/output flexibility, such as boundary stabilization by output feedback control law.
- Links with irreversible processes and the first and second laws of thermodynamics.

Port-Hamiltonian formulations for the modeling, simulation and control of fluids

Flávio Luiz Cardoso-Ribeiro^a, Ghislain Haine^b, Yann Le Gorrec^c, Denis Matignon^b, Hector Ramirez^d

^a*Divisão de Engenharia Aeronáutica e Aeroespacial, Instituto Tecnológico de Aeronáutica, São José dos Campos, 12228-900, SP, Brazil*

^b*Fédération ENAC ISAE-SUPAERO ONERA, Université de Toulouse, Toulouse, 31055, France*

^c*SUPMICROTECH, CNRS, FEMTO-ST institute, Besançon, 25000, France*

^d*Departamento de Electrónica, Universidad Técnica Federico Santa María, Valparaiso, 2390123, Chile*

Abstract

This paper presents a state of the art on port-Hamiltonian formulations for the modeling and numerical simulation of open fluid systems. This literature review, with the help of more than one hundred classified references, highlights the main features, the positioning with respect to seminal works from the literature on this topic, and the advantages provided by such a framework. A focus is given on the shallow water equations and the incompressible Navier-Stokes equations in 2D, including numerical simulation results. It is also shown how it opens very stimulating and promising research lines towards thermodynamically consistent modeling and structure-preserving numerical methods for the simulation of complex fluid systems in interaction with their environment.

Keywords: energy-based modeling, port-Hamiltonian systems, structure-preserving discretization, boundary control, shallow water equations, incompressible Navier-Stokes equations

1 Introduction

2 Port-Hamiltonian (pH) systems formulations are an extension of Hamilto-
3 nian formulations initially proposed in the context of classical mechanics for
4 closed systems to model open physical systems. These energy-based formu-
5 lations encode through a well-defined geometric structure the links existing

6 between the dynamics of the energy variables, the thermodynamic driving
7 forces, the energy function and the environment using the notion of ports
8 of interaction. They are then particularly well suited for the modular mod-
9 elling of complex multi-physics systems. These formulations have recently
10 been generalized to distributed parameters systems in [126] defining the no-
11 tion of boundary port variables from the evaluation of the co-states variables
12 at the boundary of the spatial domain. They have been extensively used
13 in continuous mechanics to model flexible / compliant structures such as
14 beams or plates. Their application to the modelling of fluids, as systems
15 with possible interactions with the environment through open flows or fluid
16 structure interactions is more recent but has shown to be very interesting for
17 both modeling and simulation purposes in various fields of application such
18 as aeronautics, acoustics, microfluidic systems, process control. There are
19 indeed a lot of structure-preserving numerical schemes that have been devel-
20 oped to preserve the energy balances and to avoid the numerical stiffness due
21 to the interdomain couplings between different subsystems. In this paper,
22 we give an overview of these recent results, focusing on their applications to
23 fluid dynamics in general and to some well-known application cases such as
24 shallow water equations or incompressible Navier-Stokes equations. We also
25 give some open research lines that are currently investigated in this field of
26 research.

27 The paper is organized as follows: a comprehensive state of the art is pre-
28 sented in § 1, with an emphasis on structure-preserving numerical methods
29 for partial differential equations (PDE). Then, in § 2, pH modeling in fluids
30 mechanics is addressed: a general setting is presented and possible extensions
31 to dissipative pH systems are introduced; moreover two motivating examples
32 are treated, which will be of interest throughout the paper, the shallow wa-
33 ter equation (SWE) in § 2.3 and the incompressible Navier-Stokes equation
34 (NSE) in § 2.4. In § 3, the structure-preserving discretization method called
35 Partitioned Finite Element Method (PFEM) is detailed on the worked out
36 example of the 2D SWE, in the irrotational and non-dissipative case; then it
37 is shown how dissipation can be taken into account at the discrete level in a
38 structure-preserving manner; finally, the control of the 2D SWE by boundary
39 feedback helps illustrate the effectiveness of the approach. The example of
40 the 2D incompressible NSE is presented as a more difficult example, and first
41 rephrased into a linear pH system, when the choice is made to describe it with
42 vorticity as energy variable, and stream function as co-energy variable; con-
43 vincing numerical results are provided for 3 different values of the Reynolds

44 number on the benchmark of the lid-driven cavity problem. Finally, in § 4, an
45 extension of the approach, including thermodynamics, is addressed: first in
46 § 4.1, quasi pH systems are presented, when the dynamical system depends
47 on the co-energy variables instead of a modulation by the energy variables;
48 finally in § 4.2, the formalism of irreversible pH system is introduced.

49 1. State of the art

50 Since the topic addressed in this review paper bears strong links with
51 several scientific fields, the comprehensive review will be organized under the
52 following scientific themes of interest: some cornerstone publications on pH
53 systems will be presented first, immediately followed by a list of worked-out
54 applications of this approach. Then, the focus will be made on Hamiltonian
55 formulations available in fluid mechanics. The most detailed part is devoted
56 to so-called compatible discretization. Finally, some links to thermodynamics
57 are provided.

58 *Port-Hamiltonian systems.* A complete and comprehensive framework for
59 modeling the dynamics of complex interconnected systems as pH systems
60 can be found first in [43] and later in [125]: in both these books, infinite-
61 dimensional systems are tackled, but not only. The seminal paper that
62 presents distributed-parameter systems as pH systems for the first time is
63 [126]; since then, many extensions and novelties have been explored, which
64 are extensively traced back in the literature review paper [116]. In par-
65 ticular, this approach is based on *Hamiltonian systems* for closed physical
66 systems, see [106], and on the abstract notion of *Dirac structures*, defined in
67 [38], for open physical systems. One of the main properties of pH systems
68 is their invariance under **power-conserving** interconnection, detailed in [34].
69 The particular 1D case has been fully understood from the original work [83],
70 dissipation has been taken into account in [138] thanks to the introduction of
71 extra dissipative ports, and [73] is a monograph on the 1D linear case: exist-
72 ence, uniqueness and regularity results are given in these references. For the
73 nD case, such theoretical results can be found in [80] for the wave equation,
74 a generalization to other first-order operators linear systems is proposed in
75 [132], and a generalization to first- and second-order operators linear systems
76 encompassing the previous one can be found in [22]; a more abstract setting
77 via system nodes is provided in [111]. In particular in 2D, the geometric
78 setting has been extended to tensor-valued functionals, see [18]. In [140],

79 the symmetry reduction of a pH system is proved to give rise to another pH
80 system in a smaller space dimension, which is another very interesting prop-
81 erty of pH system for the modeling of multiscale systems. **Preserving the pH**
82 **structure through Model Order Reduction also proves possible, as has been**
83 **studied, for instance in [63]; a more recent work in this direction, focusing**
84 **on the realization of pH systems in a data-driven manner can be found in**
85 **[12].** Finally, note that the link between infinite-dimensional pH systems and
86 the GENERIC¹ framework, which helps encode the first and second laws of
87 thermodynamics, has been given in [102, 86].

88 *Some worked-out examples.* Many references put forward the interest of the
89 modular approach enabled by pH systems: let us mention [5] for a rotating
90 flexible spacecraft, or [141] for the dynamics of complex mechanical struc-
91 tures where, typically, subsystem dynamics can be formulated in a domain-
92 independent way and interconnected by means of power flows. In [70], the 1D
93 longitudinal vibrations of a nanorod are modelled as a differential-algebraic
94 pH system. Now, the reader interested in examples involving fluid mechanics
95 models will have quite a wide choice also: the 1D SWE has been presented
96 in [69] and [68] where a network of irrigation channels is modelled and con-
97 trolled by interconnection, an extension to 2D can be found in [108], using
98 the language of exterior calculus and differential forms. The 2D SWE has
99 also been studied in [28] together with boundary control of a circular water
100 tank. Coupled systems of Fluid-Structure Interaction (FSI) have been ex-
101 tensively studied in 1D in [32] for a liquid sloshing in a moving container,
102 then generalized in 2D in [33]; note that these latter works use vector cal-
103 culus, in many available coordinate systems, instead of exterior calculus. In
104 [4] one can find a derivation of the 1D NSE coupled with chemical reactions.
105 Moreover, quite a number of examples are applied either to vocal folds, see
106 *e.g.* [97], [98], or to musical instruments, typical for multi-physics problem,
107 see *e.g.* [87] where the jet interacting with the brass player’s lip is modelled
108 as a pH system, and also [120] where the guitar is modelled as a pH system
109 resulting from FSI. A careful derivation of a poro-elastic model can be found
110 in [3]. The thermo-magneto-hydrodynamics (TMHD) interdomain couplings
111 is studied in depth in [105] for plasma high confinement in Tokamaks.

¹the acronym stands for *General Equation for the Non-Equilibrium Reversible-Irreversible Coupling*

112 *Hamiltonian formulations in fluid mechanics.* The solutions to systems of
113 PDEs such as the NSE satisfy strong constraints, which reflect the under-
114 lying mathematical structure of the equations (*e.g.*, Hamiltonian structure,
115 Poisson structure, de Rham sequence). The seminal paper on such a struc-
116 tured viewpoint is [101]. **The modelling of gas flow, based on the Euler**
117 **equations, is fully reported in e.g. [41].** A first description of NSE as a pH
118 system can be found in 1D in [4], and in ND in [96]. A more geometric-
119 oriented description of the NSE has been proposed in [25], a work based
120 on the companion papers [117, 118]. Recently, the same authors introduced
121 an extension of their framework to thermodynamics with an application to
122 Fourier-Navier-Stokes fluid in [27], and also to FSI in [26]. All these works are
123 based on the classical derivation of the equations of fluid mechanics, which
124 can be found in the monographs [35] and [16].

125 *Compatible discretization.* One of the best expositions of this central topic
126 can be found in [142]: *In recent years, there has been an increasing in-*
127 *terest in the various aspects of structure preservation at the discrete level.*
128 *This interest is rooted in three important points. First, there are well-known*
129 *connections between discrete structure preservation and standard properties*
130 *of numerical methods. Second, standard properties only guarantee physical*
131 *fidelity in the limit of fully (at least highly) resolved discretizations. Reaching*
132 *this limit requires infeasible computational resources. In contrast, structure-*
133 *preserving discretizations, by construction, generate solutions that satisfy the*
134 *underlying physics even in highly under-resolved simulations. This is ex-*
135 *remely relevant since most (if not all) simulations are inherently under-*
136 *resolved. Third, physics preservation is fundamental when coupling sys-*
137 *tems in multi-physics problems. The underlying principle behind structure-*
138 *preserving discretizations is to construct discrete approximations that retain*
139 *as much as possible the structure of the original system of PDEs. A depar-*
140 *ture from this principle introduces spurious nonphysical modes that pollute*
141 *the physics of the system being modeled.*

142 General presentation of this topic can be found in [14] and [71]. With this
143 main concern of compatible discretization at stake, many different flavors
144 have been presented: the first structure-preserving discretization scheme for
145 distributed pH systems was proposed by [60], where the authors proposed
146 a mixed finite element method for the 1D wave equation; the method used
147 a low-order Whitney bases function and was based on exact satisfaction of
148 the strong-form equations in the corresponding spanned finite-dimensional

149 approximation spaces. Based on this, [109] presented a structure-preserving
150 numerical scheme for the nonlinear SWE, which proves useful since both mass
151 and energy are preserved at the discrete level. An extension of this method
152 to use the higher order pseudo-spectral polynomial approximation basis was
153 then proposed by [103], and the Bessel function was used by [139]. A similar
154 idea was considered by [50, 52, 51] for the 1D linear transmission line and
155 the Maxwell equations. There, one equation was kept in the strong form,
156 and the other in the weak form. All these previous methods, which rely on
157 finding compatible bases that exactly satisfy at least one of the equations in
158 strong form, are relatively straightforward to apply for 1D equations. How-
159 ever, they seem cumbersome for higher dimension. Using rather the weak
160 form of both equations, and two different types of basis functions for flows
161 and efforts were studied in [77] and applied for the 2D wave equation, re-
162 quiring a projection in the very last step. A comprehensive overview of this
163 type of method can be found in the monograph [76]. An adaptation of the
164 finite difference method to pH systems both in 1D and 2D can be found in
165 [135], where the pH framework is combined with finite differences on stag-
166 gered grids to derive control oriented reduced order systems for the 2D wave
167 equation.

168 Discrete exterior calculus (DEC), see [94] and references therein, has been
169 applied to pH system in [131]. Finite element exterior calculus (FEEC), with
170 the seminal papers [7, 6], has recently been applied to pH system in [24], also
171 inspired by the dual-field mixed weak formulation introduced in [142]. The
172 primal-dual setting is also a key point in [134]. And a full review of the sub-
173 ject of compatible finite elements for geophysical fluids can be found in [37].
174 More recently, another approach has developed a discretization of the physi-
175 cal field laws based on discrete variational principles: this approach has been
176 used in the past to construct variational integrators for Lagrangian systems,
177 see e.g. [54]. Also, structure-preserving schemes applied to the GENERIC
178 framework have been explored by [78]. Tackling dissipative evolution equa-
179 tions in a structure-preserving way has been studied by [46].

180 In a nutshell, the Partitioned Finite Element Method (PFEM) is based on
181 the mixed finite elements method for first-order coupled systems, an integra-
182 tion by parts or the appropriate Stokes formula to make the boundary control
183 appear naturally, and also the finite element method to take into account the
184 constitutive relations linking energy variables to co-energy variables; it comes
185 along with sparse matrices which might help a lot for the scientific comput-
186 ing aspect. Thus, this method is based on classical applied mathematics

187 theories, which are fully developed in the monographs [59] and [15]. A first
188 global presentation of the PFEM can be found in [30]. The PFEM has al-
189 ready enjoyed many successful examples where the dynamics is linear and
190 the Hamiltonian quadratic: the 2D wave equation [130], an extension to the
191 damped case [128], the n D heat equation [129], the 3D or 2D Maxwell equa-
192 tions [110, 66], the Reissner-Mindlin plate [18], the Kirchhoff-Love plate [19]
193 for example. The extension to some implicit pH system, like the Dzekter
194 seepage model in 2D or the nanorod in 1D, are to be found in [9]. When
195 mixed boundary controls are to be taken into account, different adaptations
196 of the PFEM can be used, see [20], or [21] for the use of the Hellinger-Reissner
197 principle. Note that a full characterization of the optimal choice of finite ele-
198 ments families based on the numerical analysis of the scheme, together with
199 worked out simulation results for the 2D wave equation on different geome-
200 tries, is available in [67]; in particular, the importance of the discrete de
201 Rham complex is enlightened. As a convincing example of the advantage of
202 developing structure-preserving numerical methods for coupled sub-systems,
203 one can cite [65], in which some refined asymptotics, that were predicted
204 theoretically at the continuous level, can be recovered at the discrete level.
205 However, the application of the PFEM to fluid mechanics requires some care,
206 since the dynamical system is intrinsically non-linear: nevertheless, as will
207 be detailed in this paper, it can be extended to these models, either when
208 the non-linear relation proves of polynomial nature [28], or when the consti-
209 tutive relation, though linear, becomes of differential nature [64]. Last, but
210 not least, the PFEM comes along with a user guide [23, 53], and the source
211 codes are made available at <https://g-haine.github.io/scrimp/>. In this
212 respect, a useful benchmark on numerical models for pHs can be found at
213 <https://algopaul.github.io/PortHamiltonianBenchmarkSystems.jl/>.

214 *About Differential Algebraic Equations.* In the classical energy-coenergy for-
215 mulation of pH system, the dynamic equations are supplemented by the
216 so-called constitutive relations, which do play the role of constraints. As
217 far as coupling is concerned in modeling civil engineering structures, a rep-
218 resentation of the interconnected systems is used to generate coupling con-
219 straints, which leads to differential algebraic equations (DAEs) of index at
220 most two. [79] is one of the first monographs on these kinds of equations.
221 Infinite-dimensional setting for DAE has been tackled in [82], while the pH
222 formulation has been studied in [40]. A strong link between pHs and DAEs
223 has been fully detailed in [124]. The general definition of so-called finite-

224 dimensional descriptor pH system followed in [8]. [122] provides a closer look
225 at such systems with many examples, and in particular both the Lagrange
226 subspace and Dirac structure are introduced. The works [137], [91] and re-
227 cently [92] testify of the specific interest in dissipative pH-DAEs, which are
228 more likely to appear in the modeling of real-world processes. A full review
229 on the subject of DAEs has been published in [90]. Recently, there has been
230 a renewed interest in infinite-dimensional DAEs with the question of solvabil-
231 ity addressed in [72], the Weierstraß canonical form in [48], and the notion
232 of index in [49].

233 *The role of thermodynamics.* In numerous physical scenarios, thermal as-
234 pects and irreversible thermodynamic processes play a crucial role. This
235 is particularly evident in heat transfer, chemical reactions and reacting flu-
236 ids, among others [39, 13]. The dissipative pH system formulation can fall
237 short in these instances, necessitating the integration of heat or entropy bal-
238 ance equations into the models. Modeling, simulation and control challenges
239 in chemical engineering are notably complex due to nonlinearities arising
240 from thermodynamic properties and flux relationships [42]. A promising
241 method for creating non-linear controllers involves leveraging the charac-
242 teristics of dynamical models based on fundamental principles. These in-
243 clude symmetries, invariants, and balance equations related to specific ther-
244 modynamic potentials, like entropy. In many fluid systems, these balance
245 equations have been effectively applied as dissipation inequalities [36, 68] in
246 passivity-based control schemes, now a well-established area of study [43].
247 For chemical processes, different thermodynamic potentials such as the en-
248 tropy or Helmholtz free energy are considered in designing controllers based
249 on Lyapunov functions and passivity [2]. However, developing constructive
250 structure preserving methods for numerical approximations in this context
251 remains a challenge. Several types of “thermodynamic” dynamical models
252 have been proposed, aiming to account for both energy conservation and ir-
253 reversible entropy production. These include pseudo-gradient systems [96],
254 which are redefined with a pseudo-metric, similar to the approach for elec-
255 trical circuits in [17]. Other types include metriplectic systems such as the
256 General Equation for the Non-Equilibrium Reversible-Irreversible Coupling
257 GENERIC [62, 107, 61], nonlinearly constrained Lagrangian systems [93, 55],
258 and implicit Hamiltonian control systems [115, 114, 104, 44], defined on sub-
259 manifolds of thermodynamic phase spaces or their symplectic extensions, and
260 controlled by systems on contact manifolds or their symplectizations [123].

261 More recently a non-linear extension of pH systems with a clear underlying
 262 geometric structure has been proposed to cope with both the first and second
 263 laws of Thermodynamics, namely Irreversible pH (IpH) systems [115, 114].

264 **2. Port-Hamiltonian modeling of fluid mechanics**

265 *2.1. General setting*

In what follows, we consider fluids filling a spatial domain denoted Ω defined by the spatial coordinate $\boldsymbol{\zeta}$ and boundary $\partial\Omega$. We denote by $H(\Omega)$ the Sobolev space of weakly differentiable functions, and by $\mathcal{X} \subset H(\Omega)$, the space of state variables. Infinite-dimensional pH systems formulation consists in writing balance equations on extensive variables of thermodynamics, *i.e.* the energy variables, as a function of the corresponding intensive variables of thermodynamics, *i.e.* the co-energy variables, derived from the variational derivative of the energy. When the constitutive relations linking the state and co-state variables are linear, and when only conservative phenomena are considered, it leads to a system of PDEs of the form $\partial_t \boldsymbol{x}(\boldsymbol{\zeta}, t) = \mathcal{J} \delta_{\boldsymbol{x}} \mathcal{H}$ where $\boldsymbol{x}(\boldsymbol{\zeta}, t) \in \mathcal{X}$ is the state, \mathcal{J} is a formally skew symmetric differential operator defined over Ω and \mathcal{H} the total energy of the system defined by:

$$\mathcal{H} := \int_{\Omega} \mathcal{H}(\boldsymbol{x}) \, d\Omega, \quad (1)$$

266 where $\mathcal{H} : \mathcal{X} \rightarrow L^1(\Omega, \mathbb{R})$ is the energy density. PH formulations also allow
 267 to explicit, in the case of open physical systems, the links existing between
 268 the dynamics of the system, the energy and the power flow at the boundary
 269 of the spatial domain, as stated in Definition 1.

Definition 1. *A distributed-parameter pH system is defined by the set of PDEs and boundary port variables defined by:*

$$\partial_t \boldsymbol{x}(\boldsymbol{\zeta}, t) = \mathcal{J} \delta_{\boldsymbol{x}} \mathcal{H}, \quad (\text{or } \boldsymbol{f} = \mathcal{J} \boldsymbol{e}), \quad (2)$$

$$\begin{pmatrix} \boldsymbol{f}_{\partial} \\ \boldsymbol{e}_{\partial} \end{pmatrix} = \mathcal{W}_{\partial\Omega} \delta_{\boldsymbol{x}} \mathcal{H}, \quad (3)$$

where \mathcal{J} is a formally skew-symmetric differential operator, known as the structure (matrix) operator, $\boldsymbol{f}_{\partial}$ and $\boldsymbol{e}_{\partial}$ are the boundary flow and effort port variables, $\mathcal{W}_{\partial\Omega}$ is an operator that is related to the normal and tangential

projections on $\partial\Omega$ of the co-energy variables $\mathbf{e} := \delta_{\mathbf{x}}\mathcal{H}$ induced by \mathcal{J} such that:

$$\dot{\mathcal{H}} = \int_{\partial\Omega} \mathbf{f}_{\partial} \cdot \mathbf{e}_{\partial} \, d\gamma, \quad (4)$$

270 where $\dot{\mathcal{H}}$ denotes the time derivative of the Hamiltonian, and $\int_{\partial\Omega} \mathbf{f}_{\partial} \cdot \mathbf{e}_{\partial} \, d\gamma$
 271 describes the power supplied to the system through the boundaries².

272 From a geometrical point of view, $(\mathbf{f}, \mathbf{e}, \mathbf{f}_{\partial}, \mathbf{e}_{\partial}) \in \mathcal{D}$ at any time $t > 0$, where
 273 \mathcal{D} is a Dirac structure³.

274 From (4) one can see that the total energy of the system is constant
 275 along the state trajectories as soon as the boundary port variables are set
 276 to zero, *i.e.* when the system is closed with respect to energy. This reflects
 277 the fact that the considered system is conservative, and balance equations
 278 reduce to a system of conservation laws. When the system is subject to
 279 internal dissipation, as it is the case for fluids with viscous damping, it is
 280 possible to extend the Dirac structure with some dissipative ports associated
 281 to dissipative closure relations as detailed in the next section. An alternative
 282 approach that will be discussed in Section 4 is to include in the system
 283 description the thermal domain. PH formulations have also been recently
 284 extended to systems with constraints or implicit definitions of the energy
 285 in [89]; **boundary-implicit port-Hamiltonian systems have been thoroughly**
 286 **treated in the thesis [99].**

287 2.2. Dissipative port-*Hamiltonian* systems

288 As it is the case for finite-dimensional systems, infinite-dimensional pH
 289 formulations initially proposed to represent conservative systems have been
 290 extended in [138] to systems with dissipation of the form $\partial_t \mathbf{x}(\zeta, t) = \mathcal{J} \delta_{\mathbf{x}} \mathcal{H} -$
 291 $\mathcal{G} S \mathcal{G}^* \delta_{\mathbf{x}} \mathcal{H}$, where \mathcal{G} is a differential operator and \mathcal{G}^* the corresponding formal
 292 adjoint, and $S \geq 0$ is a non-negative bounded matrix operator of appropriate
 293 dimensions. In this case, $\mathcal{G} S \mathcal{G}^*$ represents the dissipation and can be split
 294 into two parts such as to extend the Dirac structure, as stated in Definition 2.

²In this work, we will always assume a strong regularity (*i.e.* at least C^1 in space and time) for the solutions to a pH system. In this case, the boundary traces of such solutions are then sufficiently regular to allow the identification of the duality bracket at the boundary of Ω with the L^2 -inner product at the boundary.

³Some useful definitions are recalled in Appendix A, see also *e.g.* [83]

Definition 2. A distributed-parameter dissipative pH system is defined by the set of PDEs and boundary port variables defined by:

$$\begin{pmatrix} \partial_t \mathbf{x}(\boldsymbol{\zeta}, t) \\ \mathbf{f}_d \end{pmatrix} = \underbrace{\begin{bmatrix} \mathcal{J} & \mathcal{G} \\ -\mathcal{G}^* & 0 \end{bmatrix}}_{\tilde{\mathcal{J}}} \begin{pmatrix} \mathbf{e} \\ \mathbf{e}_d \end{pmatrix}, \text{ with } \mathbf{e}_d = S \mathbf{f}_d, \quad (5)$$

$$\begin{pmatrix} \mathbf{f}_\partial \\ \mathbf{e}_\partial \end{pmatrix} = \tilde{\mathcal{W}}_{\partial\Omega} \begin{pmatrix} \mathbf{e}|_{\text{d}\Omega} \\ \mathbf{e}_d|_{\text{d}\Omega} \end{pmatrix}, \quad (6)$$

where $\partial_t \mathbf{x}(\boldsymbol{\zeta}, t) \in \mathcal{F}$ and $S > 0$. $\tilde{\mathcal{J}}$ is an extended formally skew-symmetric differential operator, \mathbf{f}_∂ and \mathbf{e}_∂ are the boundary flow and effort port variables, $\tilde{\mathcal{W}}_{\partial\Omega}$ is an operator induced by $\tilde{\mathcal{J}}$, that is related to the normal and tangential projections on $\partial\Omega$ of the co-energy variables $\mathbf{e} := \delta_{\mathbf{x}} \mathcal{H}$ and dissipative effort \mathbf{e}_d , such that:

$$\dot{\mathcal{H}} = \int_{\partial\Omega} \mathbf{f}_\partial \cdot \mathbf{e}_\partial \, \text{d}\gamma - \int_{\Omega} \mathbf{f}_d \cdot \mathbf{e}_d \, \text{d}\Omega \leq \int_{\partial\Omega} \mathbf{f}_\partial \cdot \mathbf{e}_\partial \, \text{d}\gamma, \quad (7)$$

295 where $\int_{\partial\Omega} \mathbf{f}_\partial \cdot \mathbf{e}_\partial \, \text{d}\gamma$ describes the power supplied to the system through the
 296 boundaries and $\int_{\Omega} \mathbf{f}_d \cdot \mathbf{e}_d \, \text{d}\Omega$ the power dissipated into heat by the internal
 297 phenomena (such as friction or viscosity).

298 2.3. Example of shallow water equations

299 The SWE are among the most researched fluid dynamical problems within
 300 the pH framework. These non-linear, wave-like equations have found appli-
 301 cations in various domains. They have been employed, for example, to model
 302 free-surface fluids in water channels (see, for instance, [108, 69, 68]), as well
 303 as for simulating and controlling fluids in moving tanks and fluid-structure
 304 systems (see [32, 33]).

305 In this subsection, we aim to provide a clear and pedagogical exposition
 306 of the 1D SWE within the context of the pH framework, which can be found
 307 in § 2.3.1. Subsequently, we extend our discussion to the 2D version of these
 308 equations, presented in § 2.3.2.

309 2.3.1. 1D SWE

310 The 1D SWE are nonlinear PDEs, typically written as two conservation
 311 laws, the first one models the conservation of mass, while the second one

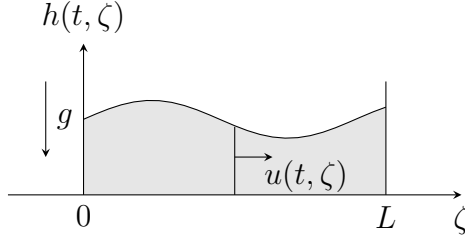


Figure 1: The one-dimensional shallow water equation.

312 model the conservation of linear momentum:

$$\begin{cases} \partial_t h = -\partial_\zeta (hu) , \\ \partial_t u = -\partial_\zeta \left(\frac{u^2}{2} + gh \right) , \end{cases} \quad (8)$$

313 where $h(\zeta, t)$ is the fluid height, $u(\zeta, t)$ the fluid average velocity in a cross-
 314 section, ζ the spatial coordinate, t the time and g the gravitational accel-
 315 eration, see Figure 1 for a schematic view of the different variables in play.

316

317 The total energy \mathcal{T} of the system inside the 1D domain $\Omega = [0, L]$ is given
 318 by the sum of kinetic and potential (gravitational) energy:

$$\mathcal{T} = \frac{1}{2} \int_{[0,L]} (\rho b h u^2 + \rho b g h^2) d\zeta , \quad (9)$$

319 where b is the width of the water channel (or fluid tank) and ρ the fluid density
 320 (assumed to be a constant). Defining the energy variables $q(\zeta, t) := bh(\zeta, t)$
 321 and $\alpha(\zeta, t) := \rho u(\zeta, t)$, the system Hamiltonian (total energy) is given by:

$$\mathcal{H} [q(\zeta, t), \alpha(\zeta, t)] = \frac{1}{2} \int_{[0,L]} \left(\frac{q\alpha^2}{\rho} + \frac{\rho g}{b} q^2 \right) d\zeta . \quad (10)$$

322 Using these newly defined variables, (8) can be rewritten as⁴:

$$\begin{pmatrix} \partial_t q \\ \partial_t \alpha \end{pmatrix} = \underbrace{\begin{pmatrix} 0 & -\partial_\zeta \\ -\partial_\zeta & 0 \end{pmatrix}}_{\mathcal{J}} \begin{pmatrix} e_q \\ e_\alpha \end{pmatrix} , \quad (11)$$

⁴In this case, $\mathcal{J} : H^1(\Omega) \times H^1(\Omega) \subset L^2(\Omega) \times L^2(\Omega) \rightarrow L^2(\Omega) \times L^2(\Omega)$ is indeed formally skew-symmetric, thanks to integration by parts, see Appendix A.

323 where $e_q(\zeta, t)$ and $e_\alpha(\zeta, t)$ are the co-energy variables (respectively, the total
 324 pressure and the water flow) which are defined as the variational derivatives
 325 of the Hamiltonian with respect to $q(\zeta, t)$ and $\alpha(\zeta, t)$:

$$\begin{cases} e_q := \frac{\delta \mathcal{H}}{\delta q} = \frac{\alpha^2}{2\rho} + \frac{\rho g}{b} q = \rho \left(\frac{u^2}{2} + gh \right), \\ e_\alpha := \frac{\delta \mathcal{H}}{\delta \alpha} = \frac{q\alpha}{\rho} = bhu. \end{cases} \quad (12)$$

326 Finally, from the time-derivative of the Hamiltonian (10) along the tra-
 327 jectories constrained to (11), one obtains the following power balance:

$$\begin{aligned} \dot{\mathcal{H}} &= \int_{[0,L]} (e_q(\zeta, t)\dot{q}(\zeta, t) + e_\alpha(\zeta, t)\dot{\alpha}(\zeta, t)) \, d\zeta, \\ &= - \int_{[0,L]} \frac{\partial}{\partial \zeta} (e_q(\zeta, t)e_\alpha(\zeta, t)) \, d\zeta, \\ &= - \int_{\partial[0,L]} e_q(\zeta, t)e_\alpha(\zeta, t) \, d\zeta, \\ &= \mathbf{e}_\partial^T \mathbf{f}_\partial, \end{aligned} \quad (13)$$

328 where the effort boundary ports, \mathbf{e}_∂ , are defined as the values of the co-energy
 329 variable e_α evaluated in the spatial domain boundary:

$$\mathbf{e}_\partial := \begin{pmatrix} e_\alpha(0, t) \\ e_\alpha(L, t) \end{pmatrix}, \quad (14)$$

330 while the power-conjugate flow boundary ports \mathbf{f}_∂ are defined as:

$$\mathbf{f}_\partial := \begin{pmatrix} e_q(0, t) \\ -e_q(L, t) \end{pmatrix}. \quad (15)$$

331 **Remark 1.** Equations (11), together with the Hamiltonian (10) and the co-
 332 energy variables (12) and boundary effort/flow (14), (15) definitions, describe
 333 a distributed-parameter pH system as presented in Definition 1, with $\mathbf{x} :=$
 334 $\begin{pmatrix} q \\ \alpha \end{pmatrix}$ as state.

335 Furthermore, one may identify the distributed flow $\mathbf{f} := \begin{pmatrix} \partial_t q \\ \partial_t \alpha \end{pmatrix}$ and effort
 336 $\mathbf{e} := \begin{pmatrix} e_q \\ e_\alpha \end{pmatrix}$ variables, together with the boundary ports \mathbf{f}_∂ and \mathbf{e}_∂ . They

337 belong to a Dirac structure \mathcal{D} , i.e. $(\mathbf{f}, \mathbf{e}, \mathbf{f}_\partial, \mathbf{e}_\partial) \in \mathcal{D}$ at any time $t > 0$,
 338 which is generated by the structure operator \mathcal{J} and the boundary variables.

339 **Remark 2.** The effort/flow boundary ports, defined in (14) and (15) repre-
 340 sent one possible choice of boundary ports as defined in the general setting (3).
 341 The choices made here exhibit a clear physical meaning: they represent the
 342 fluid total pressure and volumetric flow at the boundaries (such that their
 343 product represents the power that flows through the boundary). Obviously,
 344 only one of these ports can be imposed at a given time. Typically, from a
 345 control perspective, these variables are written as input and output (observ-
 346 ation) variables (since one of them is imposed as a control input, and the
 347 other is an output).

348 **Remark 3.** It is possible to modify (11) to introduce a distributed dissipa-
 349 tion function. The friction of the fluid with the channel bottom is usually
 350 introduced as a force e_d distributed along the fluid:

$$\underbrace{\begin{pmatrix} \partial_t q \\ \partial_t \alpha \end{pmatrix}}_{\partial_t \mathbf{x}} = \underbrace{\begin{pmatrix} 0 & -\partial_\zeta \\ -\partial_\zeta & 0 \end{pmatrix}}_{\mathcal{J}} \underbrace{\begin{pmatrix} e_q \\ e_\alpha \end{pmatrix}}_{\mathbf{e}} + \begin{pmatrix} 0 \\ e_d \end{pmatrix}, \quad (16)$$

where e_d is proportional and opposite to the fluid momentum, i.e. $e_d = -S e_\alpha$.
 Thus, defining $f_d := -e_\alpha$, we can recast this dissipative version of the SWE
 as:

$$\begin{pmatrix} \partial_t \mathbf{x}(\zeta, t) \\ f_d \end{pmatrix} = \underbrace{\begin{bmatrix} \mathcal{J} & 1 \\ -1 & 0 \end{bmatrix}}_{\tilde{\mathcal{J}}} \begin{pmatrix} \mathbf{e} \\ e_d \end{pmatrix}, \quad \text{with } e_d = S f_d. \quad (17)$$

351 It is straightforward to verify that the power balance is given by:

$$\begin{aligned} \dot{\mathcal{H}} &= - \int_{[0,L]} f_d e_d \, d\zeta + \mathbf{e}_\partial^T \mathbf{f}_\partial, \\ &= - \int_{[0,L]} S f_d^2 \, d\zeta + \mathbf{e}_\partial^T \mathbf{f}_\partial \leq \mathbf{e}_\partial^T \mathbf{f}_\partial. \end{aligned} \quad (18)$$

352 Consequently, the equations (17) together with the system Hamiltonian
 353 and boundary ports, define a distributed-parameter dissipative pH system as
 354 presented in Definition 2.

355 The definition of S , which can be a nonlinear function of the energy vari-
 356 ables q and α , such as $S = S(q, \alpha) \geq 0$ lead to different water-bed friction
 357 models that are commonly found in the SWE literature. For instance, the
 358 Darcy-Weisbach model is such that $S = \frac{f_{DW}b|\alpha|}{8q}$, where f_{DW} is an empirically
 359 obtained friction coefficient (see, for instance, [81, Sec. 7.2.6]).

360 In addition, a dissipation model related to fluid viscosity can also be ob-
 361 tained, as we recently presented in [29].

362 2.3.2. 2D SWE

363 Similarly, in a 2D setting, the frictionless SWE can be written as⁵:

$$\begin{pmatrix} \partial_t h \\ \partial_t \boldsymbol{\alpha} \end{pmatrix} = \underbrace{\begin{bmatrix} 0 & -\text{div} \\ -\mathbf{grad} & 0 \end{bmatrix}}_{\mathcal{J}} \begin{pmatrix} e_h \\ \mathbf{e}_\alpha \end{pmatrix}, \quad (19)$$

364 where $h(\boldsymbol{\zeta}, t)$ is the height of the fluid, $\boldsymbol{\alpha}(\boldsymbol{\zeta}, t) := \rho \mathbf{u}$ is the linear momentum,
 365 $e_h = \frac{1}{2}\rho \|\mathbf{u}\|^2 + \rho gh$ is the total pressure, $\mathbf{e}_\alpha = h\mathbf{u}$ is the volumetric flow of
 366 the fluid and $\boldsymbol{\zeta}$ is the spatial coordinate variable.

367 The total energy \mathcal{T} of the fluid is given by:

$$\mathcal{T} = \int_{\Omega} \frac{1}{2}\rho h \|\mathbf{u}\|^2 + \frac{1}{2}\rho gh^2 \, d\Omega, \quad (20)$$

368 Rewriting as a functional of the energy variables h and $\boldsymbol{\alpha}$, we can define the
 369 system Hamiltonian:

$$\mathcal{H}[h(\boldsymbol{\zeta}, t), \boldsymbol{\alpha}(\boldsymbol{\zeta}, t)] := \int_{\Omega} \frac{1}{2\rho} h \|\boldsymbol{\alpha}\|^2 + \frac{1}{2}\rho gh^2 \, d\Omega. \quad (21)$$

370 The co-energy variables are given by the variational derivative of the Hamil-
 371 tonian:

$$\begin{aligned} e_h &:= \delta_h \mathcal{H} = \frac{1}{2\rho} \|\boldsymbol{\alpha}\|^2 + \rho gh = \frac{1}{2}\rho \|\mathbf{u}\|^2 + \rho gh, \\ \mathbf{e}_\alpha &:= \delta_\alpha \mathcal{H} = h \frac{\boldsymbol{\alpha}}{\rho} = h\mathbf{u}. \end{aligned} \quad (22)$$

⁵The structure operator $\mathcal{J} : H^1(\Omega) \times H^{\text{div}}(\Omega) \subset L^2(\Omega) \times (L^2(\Omega))^2 \rightarrow L^2(\Omega) \times (L^2(\Omega))^2$ is well-defined and formally skew-symmetric thanks to Green's formula, see Appendix A.

372 The power-balance of the system can then be computed from the time-
 373 derivative of the Hamiltonian as:

$$\dot{\mathcal{H}} = \int_{\Omega} (\partial_t h e_h + \partial_t \boldsymbol{\alpha} \cdot \mathbf{e}_\alpha) \, d\Omega . \quad (23)$$

374 Then, from (19), and using Stokes theorem⁶:

$$\dot{\mathcal{H}} = \int_{\partial\Omega} e_h (-\mathbf{e}_\alpha \cdot \mathbf{n}) \, d\gamma , \quad (24)$$

375 which enables to define collocated flow and effort distributed ports along the
 376 boundary $\partial\Omega$. For example:

$$\begin{aligned} e_\partial &= -\mathbf{e}_\alpha \cdot \mathbf{n} , \\ f_\partial &= e_h , \end{aligned} \quad (25)$$

377 and the power-balance is given by a product between the flow and effort
 378 boundary ports:

$$\dot{\mathcal{H}} = \int_{\partial\Omega} e_\partial f_\partial \, d\gamma . \quad (26)$$

379 **Remark 4.** *The equations (19), together with the definitions of the sys-*
 380 *tem Hamiltonian, the co-energy variables and the boundary ports define a*
 381 *distributed-parameter pH system, as presented in Definition 1.*

382 **Remark 5.** *A modified version of (19) can be defined, that takes into account*
 383 *the (scalar) vorticity $\omega := \text{curl}_{2D} \mathbf{u} = \partial_{\zeta_1} u_2 - \partial_{\zeta_2} u_1$ of the fluid:*

$$\begin{pmatrix} \partial_t h \\ \partial_t \boldsymbol{\alpha} \end{pmatrix} = \begin{bmatrix} 0 & -\text{div} \\ -\mathbf{grad} & h^{-1} \cdot G(\omega) \end{bmatrix} \begin{pmatrix} e_h \\ \mathbf{e}_\alpha \end{pmatrix} , \quad (27)$$

384 where $G(\omega) := \rho \begin{bmatrix} 0 & 1 \\ -1 & 0 \end{bmatrix} \omega$. *Since the matrix $G(\omega)$ is skew-symmetric, it*
 385 *will play no role in the power balance (and it computes exactly as (26)).*

⁶The power flow through the boundary is a duality bracket between $H^{\frac{1}{2}}(\partial\Omega)$, $H^{-\frac{1}{2}}(\partial\Omega)$ in general. However, we assume strong solution in this work (see Remark 19), reducing this bracket to a more convenient L^2 -inner product at the boundary. More involved discussions and results about this concern may be found in *e.g.* [67, Section 2.1] or [30, Section 3.1] and the many references therein.

386 *2.4. Example of incompressible Navier-Stokes equations*

387 The NSE for a Newtonian fluid filling a domain $\Omega \subset \mathbb{R}^n$, $n = 2, 3$, com-
 388 monly read [35, 16]:

$$\begin{cases} \partial_t \rho + \operatorname{div}(\rho \mathbf{u}) &= 0, \\ \rho(\partial_t + \mathbf{u} \cdot \mathbf{grad})\mathbf{u} &= -\mathbf{grad}(P) + \mu \Delta \mathbf{u} + (\lambda + \mu) \mathbf{grad}(\operatorname{div}(\mathbf{u})), \end{cases} \quad (28)$$

389 where ρ is the mass density, \mathbf{u} is the particle velocity, P is the static pressure,
 390 $\mu > 0$ is the dynamic viscosity, and λ is related to $\eta := \lambda + \frac{2}{3}\mu$, known as the
 391 bulk viscosity, the latter being equal to 0 under Stokes assumption (in which
 392 case, $\lambda = -\frac{2}{3}\mu$).

Thanks to the identity $-\Delta = \mathbf{curl} \mathbf{curl} - \mathbf{grad} \operatorname{div}$, the linear momentum evolution rewrites:

$$\rho \partial_t \mathbf{u} = -\rho(\mathbf{u} \cdot \mathbf{grad})\mathbf{u} - \mathbf{grad}(P) - \mu \mathbf{curl}(\mathbf{curl}(\mathbf{u})) + (\lambda + 2\mu) \mathbf{grad}(\operatorname{div}(\mathbf{u})).$$

Let $\rho \mapsto e(\rho)$ be the internal energy density, and define the Hamiltonian functional as the total energy of the system:

$$\mathcal{E} := \int_{\Omega} \left(\frac{1}{2} \rho \|\mathbf{u}\|^2 + \rho e(\rho) \right) d\Omega.$$

393 Choosing the density ρ and the velocity \mathbf{u} as energy variables, one can com-
 394 pute the co-energy variables $e_{\rho} := \delta_{\rho} \mathcal{E} = \frac{1}{2} \|\mathbf{u}\|^2 + \frac{P}{\rho} = h(\rho, \mathbf{u})$ which is the
 395 *enthalpy* density, and $\mathbf{e}_{\mathbf{u}} := \delta_{\mathbf{u}} \mathcal{E} = \rho \mathbf{u}$ which is the linear momentum density.

396 Let us introduce two extra dissipation ports:

- 397 • $\mathbf{f}_c := \boldsymbol{\omega} = \mathbf{curl} \mathbf{u} = \mathbf{curl}(\rho^{-1} \mathbf{e}_{\mathbf{u}})$,
- 398 • $f_d := \operatorname{div} \mathbf{u} = \operatorname{div}(\rho^{-1} \mathbf{e}_{\mathbf{u}})$,

399 which are both physically meaningful, and add the *closure relations* $e_d =$
 400 $\mu_d f_d$ and $\mathbf{e}_c = \mu_c \mathbf{f}_c$ (with $\mu_c = \mu$ and $\mu_d = \lambda + 2\mu = \frac{4}{3}\mu$). Then, following
 401 [96], we are in a position to recast the NSE for an isentropic Newtonian fluid
 402 as a pH system.

403 **Theorem 1.** *The NSE (28) rewrites:*

$$\begin{pmatrix} \partial_t \rho \\ \partial_t \mathbf{u} \\ \mathbf{f}_c \\ f_d \end{pmatrix} = \tilde{\mathcal{J}} \begin{pmatrix} e_{\rho} \\ \mathbf{e}_{\mathbf{u}} \\ \mathbf{e}_c \\ e_d \end{pmatrix}, \quad (29)$$

404 where the interconnection differential operator $\tilde{\mathcal{J}}$ is:

$$\tilde{\mathcal{J}} = \begin{bmatrix} 0 & -\text{div} & 0 & 0 \\ -\mathbf{grad} & \rho^{-1}.G(\boldsymbol{\omega}) & -\rho^{-1}.\mathbf{curl} & \rho^{-1}.\mathbf{grad} \\ 0 & \mathbf{curl}(\rho^{-1}.) & 0 & 0 \\ 0 & \text{div}(\rho^{-1}.) & 0 & 0 \end{bmatrix}. \quad (30)$$

405 Defining as state variable $\mathbf{x} := (\rho \ \mathbf{u}^\top)^\top$, collecting the dissipative variables
 406 into vectors $\mathbf{e}_d := (\mathbf{e}_c^\top \ e_d)^\top$ and $\mathbf{f}_d := (\mathbf{f}_c^\top \ f_d)^\top$ related by the closure
 407 relation $\mathbf{e}_d = S\mathbf{f}_d$, with $S = \text{Diag}(\mu_c I_n, \mu_d)$, gives a dissipative pH system in
 408 the sense of Definition 2, provided appropriate collocated boundary controls
 409 and observations are added.

410 *Proof.* See [96, eq. (22)]. □

411 Let us now consider an incompressible fluid with constant mass density
 412 $\rho \equiv \rho_0$. The first line of (29) simplifies, and multiplying the second line by
 413 ρ_0 leads to:

$$\begin{pmatrix} \rho_0 \partial_t \mathbf{u} \\ \mathbf{f}_c \\ 0 \end{pmatrix} = \begin{bmatrix} G(\boldsymbol{\omega}) & -\mathbf{curl} & \mathbf{grad} \\ \mathbf{curl} & 0 & 0 \\ \text{div} & 0 & 0 \end{bmatrix} \begin{pmatrix} \mathbf{u} \\ \mathbf{e}_c \\ e_d \end{pmatrix}. \quad (31)$$

414 The divergence-free constraint $f_d = \text{div}(\mathbf{u}) = 0$ is ensured by the presence
 415 of a Lagrange multiplier in the dynamics, under the form $\mathbf{grad}(e_d)$, where
 416 $-e_d = P + \frac{1}{2}\rho_0 \|\mathbf{u}\|^2$ is the total pressure. Hence, the pressure is determined
 417 up to a constant in these equations, as expected for incompressible fluids. It
 418 is intrinsically an infinite-dimensional pH-DAE. The linearized Navier-Stokes
 419 model at low Reynolds number, known as Oseen PDE, deserves a specific
 420 study; the Oseen model recast in a pH setting has recently been tackled
 421 in [119]. **For the reformulation of the Navier-Stokes system and the removal**
 422 **of the pressure term, see e.g. [133] and [47], where an explicit solution formula**
 423 **for the linear case is provided.**

424 **Theorem 2.** *The kinetic energy $\mathcal{H} = \frac{1}{2} \int_{\Omega} \rho_0 \|\mathbf{u}\|^2$ satisfies the power-balance:*

$$\begin{aligned} \dot{\mathcal{H}} &= - \int_{\Omega} \mathbf{e}_c \cdot \mathbf{f}_c + \int_{\partial\Omega} (e_d \mathbf{u} \cdot \mathbf{n} - \mathbf{e}_c \cdot (\mathbf{u} \wedge \mathbf{n})), \\ &= - \int_{\Omega} \mu_c \|\boldsymbol{\omega}\|^2 + \int_{\partial\Omega} \left(\left(P + \frac{1}{2}\rho_0 \|\mathbf{u}\|^2 \right) \mathbf{u} \cdot \mathbf{n} - \mu_c \boldsymbol{\omega} \cdot (\mathbf{u} \wedge \mathbf{n}) \right). \end{aligned} \quad (32)$$

425 *Proof.* See Appendix B.1. □

426 **Remark 6.** *The negative term in (32) represents the transfer of kinetic*
 427 *energy into internal energy due to the viscosity.*

428 **Remark 7.** *The boundary power flows show that the normal velocity $\mathbf{u} \cdot \mathbf{n}$*
 429 *is available for boundary control, whether the fluid be viscous or not, while*
 430 *the viscous damping is mandatory to have access to the tangential control of*
 431 *the velocity $\mathbf{u} \wedge \mathbf{n}$, since it is multiplied by the viscous term μ_c .*

432 From now on, we only consider the 2D case. Our goal is to rewrite
 433 the initial problem given in a velocity-pressure formulation into an equiv-
 434 alent problem written in vorticity-stream function, see *e.g.* [84]. Follow-
 435 ing [35, §. 1.2], we recall that the curl_{2D} differential operator is defined by
 436 $\text{curl}_{2D}(\mathbf{v}) := \partial_{\zeta_1} v_2 - \partial_{\zeta_2} v_1$, and that the following integration by parts formula
 437 holds:

$$\int_{\Omega} \text{curl}_{2D}(\mathbf{v}) w \, d\Omega = \int_{\Omega} \mathbf{v} \cdot \mathbf{grad}^{\perp}(w) \, d\Omega + \int_{\partial\Omega} (\Theta \mathbf{v}) \cdot \mathbf{n} w \, d\gamma, \quad (33)$$

438 where⁷ $\mathbf{grad}^{\perp}(w) := \begin{pmatrix} \partial_{\zeta_2} w \\ -\partial_{\zeta_1} w \end{pmatrix}$, and Θ denotes the rotation of angle $-\frac{\pi}{2}$ in
 439 the 2D plane.

Applying curl_{2D} to the linear momentum conservation equation, the first
 line of (31), leads to the following evolution equation for the scalar vorticity
 $\omega := \text{curl}_{2D}(\mathbf{u})$:

$$\rho_0 \partial_t \omega = \text{curl}_{2D}(G(\omega) \mathbf{u}) - \mu_c \text{curl}_{2D} \mathbf{grad}^{\perp}(\omega),$$

440 where we have used $\mathbf{e}_c = \mu_c \mathbf{curl} \mathbf{u} = \mu_c \omega \mathbf{k}$ in 3D, and then $\mathbf{curl}(\omega \mathbf{k}) =$
 441 $\mathbf{grad}^{\perp}(\omega)$ in 2D (since the third component is 0). Another key point is that
 442 $\text{curl}_{2D} \mathbf{grad} \equiv 0$. This classical trick enables eliminating the total pressure
 443 e_d from the system, as a Leray projector would do.

444 Assume moreover that the velocity \mathbf{u} is fully determined by a stream
 445 function ψ , which is the case for instance if Ω is simply connected⁸; thus

⁷Care must be taken that in some references, like [106] or [101], the opposite definition for \mathbf{grad}^{\perp} is chosen. We stick to this one in order to be consistent with the formal adjoint of the curl_{2D} operator.

⁸In general, thanks to the Hodge-Helmholtz decomposition of $L^2(\Omega)$, the stream function is defined up to a divergence-free, irrotational potential.

446 there exists a potential such that $\mathbf{u} = \mathbf{grad}^\perp \psi := \begin{pmatrix} \partial_{\zeta_2} \psi \\ -\partial_{\zeta_1} \psi \end{pmatrix}$. Substituting \mathbf{u}
 447 with this definition gives in turn:

$$\rho_0 \partial_t \omega = \text{curl}_{2D} (G(\omega) \mathbf{grad}^\perp(\psi)) - \mu_c \text{curl}_{2D} \mathbf{grad}^\perp(\omega). \quad (34)$$

Proposition 3. *For all sufficiently smooth functions ψ :*

$$\begin{aligned} \text{curl}_{2D} (G(\omega) \mathbf{grad}^\perp(\psi)) &= \partial_{\zeta_1}(\omega \partial_{\zeta_2} \psi) - \partial_{\zeta_2}(\omega \partial_{\zeta_1} \psi), \\ &= \text{div}(\omega \mathbf{grad}^\perp(\psi)), \\ &=: J_\omega \psi. \end{aligned}$$

448 *Furthermore, the operator J_ω , which is modulated by the energy variable ω ,*
 449 *is formally skew-symmetric, and satisfies Jacobi identities (see e.g. [106,*
 450 *Example 7.10]).*

Proof. Let us compute:

$$G(\omega) \mathbf{grad}^\perp(\psi) = \begin{pmatrix} 0 \\ 0 \\ \omega \end{pmatrix} \wedge \begin{pmatrix} \partial_{\zeta_2} \psi \\ -\partial_{\zeta_1} \psi \\ 0 \end{pmatrix} = \begin{pmatrix} \omega \partial_{\zeta_1} \psi \\ \omega \partial_{\zeta_2} \psi \end{pmatrix} = \omega \mathbf{grad} \psi.$$

451 Applying curl_{2D} gives the claimed result.

Then, the formal skew-symmetry is obvious by integration by parts since, for all $\psi \in \mathcal{C}_c^\infty(\Omega)$:

$$\int_{\Omega} \text{div}(\omega \mathbf{grad}^\perp(\psi)) \psi \, d\Omega = - \int_{\Omega} \omega \underbrace{\mathbf{grad}^\perp(\psi) \cdot \mathbf{grad}(\psi)}_{=0} \, d\Omega.$$

452

□

453 The evolution equation (34) that replaces the initial linear momentum
 454 evolution, this induces a change in the energy variable that has to be consid-
 455 ered to write the pH system. More precisely, the Hamiltonian \mathcal{H} must now
 456 be considered as a functional of the vorticity:

$$\mathcal{H}(\omega) = \frac{1}{2} \int_{\Omega} \rho_0 \|\mathbf{u}\|^2 \, d\Omega. \quad (35)$$

457 In turn, the co-energy variable has to be computed with respect to this new
 458 energy variable.

459 **Proposition 4.** *The variational derivative $\delta_\omega \mathcal{H}(\omega)$ of \mathcal{H} is $\rho_0 \psi$.*

460 *Proof.* This can be found in [106, Example 7.10] up to the presence of ρ_0 ,
 461 which plays no role in the computation. \square

462 It is clear that the presence of ρ_0 has to be taken carefully into account.
 463 There are several ways to deal with it, but one elegant one is to include this
 464 (constant-in-time) parameter in the metric, leading to the following.

465 **Corollary 5.** *Consider the weighted L^2 -inner product $\langle u, v \rangle_{\rho_0} := \int_\Omega uv \rho_0 \, d\Omega$,
 466 then the variational derivative of \mathcal{H} , $e_\omega := \delta_\omega^{\rho_0} \mathcal{H}(\omega)$, is ψ .*

467 Thanks to these results, one can finally write the dynamical system (34)
 468 in the pH form:

$$\begin{pmatrix} \rho_0 \partial_t \omega \\ f_c \end{pmatrix} = \begin{bmatrix} J_\omega & -\text{curl}_{2D} \mathbf{grad}^\perp \\ \text{curl}_{2D} \mathbf{grad}^\perp & 0 \end{bmatrix} \begin{pmatrix} \psi \\ e_c \end{pmatrix}, \quad (36)$$

469 with $\omega = \text{curl}_{2D} \mathbf{u}$, $e_\omega = \psi$ and $e_c = \mu_c \omega$, together with the constitutive
 470 relation $e_c = \mu_c f_c$.

471 The power-balance (32) may be computed with respect to these new
 472 variables.

Theorem 6. *The evolution of the Hamiltonian along the trajectories of dy-
 namical system (36) with the closure relation is given by:*

$$\begin{aligned} \dot{\mathcal{H}} = & - \int_\Omega \mu_c \omega^2 \, d\Omega + \int_{\partial\Omega} \omega \psi \mathbf{grad}^\perp(\psi) \cdot \mathbf{n} \, d\gamma \\ & + \mu_c \int_{\partial\Omega} (\psi \mathbf{grad}(\omega) \cdot \mathbf{n} - \omega \mathbf{grad}(\psi) \cdot \mathbf{n}) \, d\gamma, \end{aligned} \quad (37)$$

473 where we can identify the tangential control $u_\tau = \mathbf{grad}(\psi) \cdot \mathbf{n}$ and the normal
 474 control $u_n = \mathbf{grad}^\perp(\psi) \cdot \mathbf{n}$.

475 *Proof.* See Appendix B.2 \square

476 **Remark 8.** *Note that both controls u_n and u_τ are available in this formu-
 477 lation. However, another term appears at the boundary in (37), namely
 478 $\mu_c \psi \mathbf{grad}(\omega) \cdot \mathbf{n}$, the physical meaning of which is not clear so far. Noticing
 479 that this can be viewed as the power flow corresponding to the boundary con-
 480 trol of ψ , which obviously requires being compatible with both controls on \mathbf{u} ,
 481 is crucial to successfully apply the PFEM, as will be enlightened in Section 3.*

482 Nevertheless, a comparison of (37) with (32) allows deducing the following
 483 property about the pressure P :

Corollary 7.

$$\int_{\partial\Omega} P \mathbf{grad}^\perp(\psi) \cdot \mathbf{n} \, d\gamma = \int_{\partial\Omega} \left(\left(\omega \psi - \frac{1}{2} \rho_0 \|\mathbf{grad}^\perp(\psi)\|^2 \right) \mathbf{grad}^\perp(\psi) \cdot \mathbf{n} + \mu_c \psi \mathbf{grad}(\omega) \cdot \mathbf{n} \right) d\gamma.$$

484 **Remark 9.** In this context, the factorization of minus the 2D scalar Lapla-
 485 cian $-\Delta = \text{curl}_{2D} \mathbf{grad}^\perp$ proves more appropriate than the usual one, namely
 486 $-\Delta = -\text{div} \mathbf{grad}$. The computation is straightforward.

487 **Remark 10.** In (36), one can get rid of the realization of dissipation thanks
 488 to dissipative ports, and find the dissipative dynamics in the classical form
 489 $\mathcal{J} - \mathcal{G}S\mathcal{G}^* = \mathcal{J} - \mathcal{R}$:

$$\rho_0 \partial_t \omega = J_\omega \psi - \mu \Delta^2 \psi, \quad \text{with} \quad \psi = \delta_\omega^{\rho_0} \mathcal{H}. \quad (38)$$

490 *Moving from (36) to (38) is not only formal, indeed one of the two equivalent*
 491 *formulations can bring advantages in some applications: for example, the*
 492 *interest of the second formulation at the numerical level has been investigated*
 493 *in the case of the 2D dissipative shallow water equations in [29]. However,*
 494 *at the theoretical level, the first formulation with $\tilde{\mathcal{J}}$ could be more beneficial,*
 495 *since the domains of the unbounded operators \mathcal{J}_ω and \mathcal{R} could not coincide,*
 496 *and make the $(\mathcal{J}_\omega - \mathcal{R})$ formulation awkward, see e.g. [111] and references*
 497 *therein.*

498 **Remark 11.** Now the 2D incompressible NSE depend wholly on 2 scalar
 499 fields, in comparison with the former velocity formulation which relied on
 500 one vector field and two scalar fields. At the discrete level, this considerably
 501 reduces the number of degrees of freedom.

502 3. Structure-preserving discretization

503 This section is devoted to the discretization of distributed pH systems in
 504 a structure-preserving way: the finite-dimensional discrete (in space) system

505 must be a pH system, and its discrete Hamiltonian should satisfy a power
 506 balance that **preserves** the continuous power balance.

507 It is recalled in Appendix A that this power balance is encoded in a
 508 (Stokes-)Dirac structure [38], which can be represented as the graph of an
 509 extended structure operator constructed from the differential operator \mathcal{J}
 510 and the boundary operators [22]. At the discrete level, it should result in
 511 two matrices M and J , the former being *symmetric*, and the latter *skew-*
 512 *symmetric*.

513 In addition to the discretization of the Stokes-Dirac structure, the con-
 514 stitutive relations require a particular attention to be consistent with the
 515 targeted discrete power balance.

516 The strategy adopted below relies on the mixed finite element method,
 517 well-established for elliptic problems, and known to be robust and efficient [59,
 518 15]. However, this approach does not allow capturing discontinuities as is,
 519 and would require further work.

520 3.1. Non-dissipative irrotational shallow water equations

521 Let us start with the Stokes-Dirac structure generated by the structure
 522 operator $\mathcal{J} = \begin{bmatrix} 0 & -\text{div} \\ -\mathbf{grad} & 0 \end{bmatrix}$, *i.e.*, for the irrotational shallow water equa-
 523 tion (19).

The weak formulation of (19) reads, for all test functions $(\varphi, \boldsymbol{\phi})$ smooth enough:

$$\begin{cases} \int_{\Omega} \partial_t h \varphi \, d\Omega = - \int_{\Omega} \text{div}(\mathbf{e}_\alpha) \varphi \, d\Omega, \\ \int_{\Omega} \partial_t \boldsymbol{\alpha} \cdot \boldsymbol{\phi} \, d\Omega = - \int_{\Omega} \mathbf{grad}(e_h) \cdot \boldsymbol{\phi} \, d\Omega. \end{cases}$$

524 The boundary control $e_\partial = -\mathbf{e}_\alpha \cdot \mathbf{n}$, defined in (25), is taken into account by
 525 performing an integration by parts on the first line, leading to:

$$\begin{cases} \int_{\Omega} \partial_t h \varphi \, d\Omega = \int_{\Omega} \mathbf{e}_\alpha \cdot \mathbf{grad}(\varphi) \, d\Omega + \int_{\partial\Omega} e_\partial \varphi \, d\gamma, \\ \int_{\Omega} \partial_t \boldsymbol{\alpha} \cdot \boldsymbol{\phi} \, d\Omega = - \int_{\Omega} \mathbf{grad}(e_h) \cdot \boldsymbol{\phi} \, d\Omega. \end{cases} \quad (39)$$

Consider three finite element families $(\varphi^i)_{i=1, \dots, N_h}$, $(\boldsymbol{\phi}^k)_{k=1, \dots, N_\alpha}$ and $(\xi^m)_{m=1, \dots, N_\partial}$ for the approximation of the h -type variables, the α -type variables and the

boundary variables respectively, as follows:

$$h(\boldsymbol{\zeta}, t) \simeq h^d(\boldsymbol{\zeta}, t) := \sum_{i=1}^{N_h} h^i(t) \varphi^i(\boldsymbol{\zeta}), \quad e_h(\boldsymbol{\zeta}, t) \simeq e_h^d(\boldsymbol{\zeta}, t) := \sum_{i=1}^{N_h} e_h^i(t) \varphi^i(\boldsymbol{\zeta}),$$

for the scalar fields,

$$\boldsymbol{\alpha}(\boldsymbol{\zeta}, t) \simeq \boldsymbol{\alpha}^d(\boldsymbol{\zeta}, t) := \sum_{k=1}^{N_\alpha} \alpha^k(t) \boldsymbol{\phi}^k(\boldsymbol{\zeta}), \quad \mathbf{e}_\alpha(\boldsymbol{\zeta}, t) \simeq \mathbf{e}_\alpha^d(\boldsymbol{\zeta}, t) := \sum_{k=1}^{N_\alpha} e_\alpha^k(t) \boldsymbol{\phi}^k(\boldsymbol{\zeta}),$$

for the vector fields, and at the boundary:

$$e_\partial(\mathbf{s}, t) \simeq e_\partial^d(\mathbf{s}, t) := \sum_{m=1}^{N_\partial} e_\partial^m(t) \xi^m(\mathbf{s}), \quad f_\partial(\mathbf{s}, t) \simeq f_\partial^d(\mathbf{s}, t) := \sum_{m=1}^{N_\partial} f_\partial^m(t) \xi^m(\mathbf{s}).$$

526 The coefficients $\square^j(t)$ of the approximation \square^d of \square are collected in a vector
527 denoted $\underline{\square}(t)$.

528 Plugging these approximations into (39) and taking the finite elements
529 families as test functions, one gets:

$$\begin{bmatrix} M_h & 0 \\ 0 & M_\alpha \end{bmatrix} \begin{pmatrix} \dot{h}(t) \\ \dot{\underline{\alpha}}(t) \end{pmatrix} = \begin{bmatrix} 0 & D \\ -D^\top & 0 \end{bmatrix} \begin{pmatrix} e_h(t) \\ \mathbf{e}_\alpha(t) \end{pmatrix} + \begin{bmatrix} B \\ 0 \end{bmatrix} e_\partial(t), \quad (40)$$

where the mass matrices on the left-hand side are defined as:

$$(M_h)_{i,j} := \int_{\Omega} \varphi^j \varphi^i \, d\Omega, \quad (M_\alpha)_{k,\ell} := \int_{\Omega} \boldsymbol{\phi}^\ell \cdot \boldsymbol{\phi}^k \, d\Omega,$$

and the differential and control matrices on the right-hand side are defined
as:

$$(D)_{k,j} := \int_{\Omega} \boldsymbol{\phi}^k \cdot \mathbf{grad}(\varphi^j) \, d\Omega, \quad (B)_{m,j} := \int_{\partial\Omega} \xi^m \varphi^j \, d\gamma.$$

530 Note that $D \in \mathbb{R}^{N_h \times N_\alpha}$ and $B \in \mathbb{R}^{N_h \times N_\partial}$ are not square matrices.

If furthermore one writes the weak form of the output f_∂ defined in (25),
one obtains:

$$\int_{\partial\Omega} f_\partial \xi \, d\gamma = \int_{\partial\Omega} e_h \xi \, d\gamma,$$

which leads once approximated with the boundary finite elements:

$$M_\partial \underline{f}_\partial(t) = B^\top \underline{e}_h(t),$$

where the boundary mass matrix is defined as:

$$(M_{\partial})_{m,\ell} := \int_{\partial\Omega} \xi^\ell \xi^m \, d\gamma.$$

531 This latter equation gathered with (40) allows one to identify the matrices
 532 representing a finite-dimensional Dirac structure:

$$\underbrace{\begin{bmatrix} M_h & 0 & 0 \\ 0 & M_\alpha & 0 \\ 0 & 0 & M_{\partial} \end{bmatrix}}_{\mathbf{M}} \begin{pmatrix} \dot{\underline{h}}(t) \\ \dot{\underline{\alpha}}(t) \\ -\dot{\underline{f}}_{\partial}(t) \end{pmatrix} = \underbrace{\begin{bmatrix} 0 & D & B \\ -D^\top & 0 & 0 \\ -B^\top & 0 & 0 \end{bmatrix}}_{\mathbf{J}} \begin{pmatrix} \underline{e}_h(t) \\ \underline{e}_\alpha(t) \\ \underline{e}_{\partial}(t) \end{pmatrix}. \quad (41)$$

533 It is clear that \mathbf{M} is symmetric positive-definite and that \mathbf{J} is skew-symmetric.
 534 Then, the graph of \mathbf{J} proves to be a Dirac structure in $\mathbb{R}^{(N_h+N_\alpha+N_\partial)^2}$ equipped
 535 with the metric induced by \mathbf{M} , see [125].

536 To achieve the structure-preserving discretization, it remains to take the
 537 constitutive relations into account, in such a way the power balance of the
 538 discrete Hamiltonian will mimic the continuous one.

At least two approaches may be used to reach our goal, which prove equivalent in the case of a polynomial (but not necessarily quadratic) Hamiltonian, as considered in this work. The first way is to define the constitutive relations at the discrete level, by making use of the gradient of the discrete Hamiltonian in the metrics induced by M_h and M_α , as it has been done, *e.g.*, in [31, Section 4.2]. On the other hand, one can directly write down the weak formulations of (22), as follows:

$$\int_{\Omega} e_h \varphi \, d\Omega = \int_{\Omega} \|\alpha\|^2 \frac{\varphi}{2\rho} \, d\Omega + \int_{\Omega} h \rho g \varphi \, d\Omega,$$

$$\int_{\Omega} \mathbf{e}_\alpha \cdot \boldsymbol{\phi} \, d\Omega = \int_{\Omega} h \alpha \cdot \frac{\boldsymbol{\phi}}{\rho} \, d\Omega.$$

The finite element approximations then lead to:

$$M_h \underline{e}_h(t) = N[\underline{\alpha}(t)] \underline{\alpha}(t) + Q_h \underline{h}(t),$$

where:

$$(Q_h)_{i,j} := \int_{\Omega} \varphi^j \rho g \varphi^i \, d\Omega, \quad (N[\underline{\alpha}(t)])_{i,\ell} := \int_{\Omega} \frac{\alpha^d}{2\rho} \cdot \boldsymbol{\phi}^\ell \varphi^i \, d\Omega,$$

and,

$$M_{\underline{\alpha}} \underline{e}_{\underline{\alpha}}(t) = Q_{\underline{\alpha}}[\underline{h}(t)] \underline{\alpha}(t),$$

where:

$$(Q_{\underline{\alpha}}[\underline{h}(t)])_{k,\ell} := \int_{\Omega} \frac{h^d}{\rho} \phi^\ell \cdot \phi^k \, d\Omega.$$

539 These may be gathered in a more compact form as:

$$\begin{bmatrix} M_h & 0 \\ 0 & M_{\underline{\alpha}} \end{bmatrix} \begin{pmatrix} \underline{e}_h(t) \\ \underline{e}_{\underline{\alpha}}(t) \end{pmatrix} = \begin{bmatrix} Q_h & N[\underline{\alpha}(t)] \\ 0 & Q_{\underline{\alpha}}[\underline{h}(t)] \end{bmatrix} \begin{pmatrix} \underline{h}(t) \\ \underline{\alpha}(t) \end{pmatrix}. \quad (42)$$

Let us define the discrete Hamiltonian \mathcal{H}^d as the evaluation of the continuous one \mathcal{H} , defined in (21), in the approximated variables, as follows:

$$\mathcal{H}^d(\underline{h}(t), \underline{\alpha}(t)) := \mathcal{H}(h^d(t, \mathbf{x}), \boldsymbol{\alpha}^d(t, \mathbf{x})) = \int_{\Omega} \left[\frac{h^d}{2\rho} \|\boldsymbol{\alpha}^d\|^2 + \frac{\rho g}{2} (h^d)^2 \right] d\Omega.$$

540 Hence, with the notations of this section, the discrete Hamiltonian \mathcal{H}^d rewrites:

$$\mathcal{H}^d(\underline{h}(t), \underline{\alpha}(t)) = \frac{1}{2} \underline{\alpha}(t)^\top Q_{\underline{\alpha}}[\underline{h}(t)] \underline{\alpha}(t) + \frac{1}{2} \underline{h}(t)^\top Q_h \underline{h}(t). \quad (43)$$

Remark 12. *As already said, the polynomial structure of the Hamiltonian is crucial in this work, as the discrete weak form of the variational derivatives of the continuous Hamiltonian turns out to be the gradient of the discrete Hamiltonian in the metric induced by the mass matrices. Indeed, compare (42) with [30, Eq. (4.25) and (4.29)]. This is indeed true, thanks to the equality:*

$$\frac{1}{2} \underline{\alpha}(t)^\top Q_{\underline{\alpha}}[\underline{h}(t)] \underline{\alpha}(t) = \underline{\alpha}(t)^\top N[\underline{\alpha}(t)]^\top \underline{h}(t),$$

541 *which would not occur if the Hamiltonian were not polynomial.*

542 *Thanks to this equality, the notations $Q_{\underline{\alpha}}[\underline{h}(t)]$ and $N[\underline{\alpha}(t)]$ indeed make*
 543 *sense, even if it is h^d and $\boldsymbol{\alpha}^d$, respectively, which appear in the definitions of*
 544 *the nonlinear matrices $Q_{\underline{\alpha}}[\underline{h}(t)]$ and $N[\underline{\alpha}(t)]$.*

545 *Two worked-out examples where the polynomial structure of the relations*
 546 *proves crucial in applying the PFEM can be found in [11] for Allen-Cahn*
 547 *model, and in [10] for the Cahn-Hilliard model.*

548 **Theorem 8.** *Let $(\underline{h}(t), \underline{\alpha}(t), \underline{e}_h(t), \underline{e}_{\underline{\alpha}}(t))$ be a trajectory, i.e., it satisfies the*
 549 *discrete system (41)–(42) for some initial data and some control $\underline{e}_{\partial}(t)$, for*

550 $t \geq 0$. Then, the discrete Hamiltonian \mathcal{H}^d defined in (43) satisfies the discrete
 551 power balance:

$$\frac{d}{dt} \mathcal{H}^d(\underline{h}(t), \underline{\alpha}(t)) = \underline{e}_\partial(t)^\top M_\partial \underline{f}_\partial(t), \quad (44)$$

552 which preserves the continuous one (26) at the discrete level.

553 *Proof.* See Appendix B.3 □

554 3.2. Tackling dissipation

555 Dissipation in the framework of pH systems has been presented in Sec-
 556 tion 2.2. It relies on an extra port $(\mathbf{f}_d, \mathbf{e}_d)$, called *dissipative*, which models
 557 the loss of energy (*i.e.*, the decay of \mathcal{H}). It has been recalled that such a
 558 port, combined with a dissipative constitutive relation linking \mathbf{e}_d to \mathbf{f}_d (*e.g.*,
 559 for linear dissipation $\mathbf{e}_d = S\mathbf{f}_d$ with $S > 0$), may be viewed as an appropri-
 560 ate decomposition of the dissipative operator $\mathcal{R} = \mathcal{G}S\mathcal{G}^*$ of the PDE under
 561 consideration.

562 The PFEM is versatile enough to consider both approaches for simula-
 563 tions, either including \mathcal{R} in the dynamics, or its decomposition $\mathcal{G}S\mathcal{G}^*$. The
 564 former is straightforward as it does not need the addition of a dissipative port,
 565 while the latter may require more attention for discretization. The choice of
 566 one or the other form depends on the desired outcomes of the numerical
 567 experiments.

Nonlinear dissipation. In this case, $\mathcal{G} \equiv \begin{bmatrix} 0 \\ I \end{bmatrix}$ (the dissipation acts on the
 linear momentum equation) and the operator generating the non-linear dis-
 sipation is considered outside the Dirac structure, *i.e.*, in the dissipative
 constitutive relation as $\mathcal{N}(h, \boldsymbol{\alpha}, \mathbf{e}_d, \mathbf{f}_d) = 0$, as presented for the 1D SWE in
 Remark 3. The dissipative port is of the same mathematical nature as the
 $\boldsymbol{\alpha}$ -type port, and can be approximated with the same finite element family
 (although this is not mandatory). Hence, this leads to the extended Dirac
 structure:

$$\begin{bmatrix} M_h & 0 & 0 & 0 \\ 0 & M_\alpha & 0 & 0 \\ 0 & 0 & M_\alpha & 0 \\ 0 & 0 & 0 & M_\partial \end{bmatrix} \begin{pmatrix} \dot{h}(t) \\ \dot{\alpha}(t) \\ f_d(t) \\ -f_\partial(t) \end{pmatrix} = \begin{bmatrix} 0 & D & 0 & B \\ -D^\top & 0 & M_\alpha & 0 \\ 0 & -M_\alpha & 0 & 0 \\ -B^\top & 0 & 0 & 0 \end{bmatrix} \begin{pmatrix} e_h(t) \\ e_\alpha(t) \\ e_d(t) \\ e_\partial(t) \end{pmatrix}.$$

This Dirac structure implies straightforwardly the following power balance:

$$\frac{d}{dt} \mathcal{H}^d(\underline{h}(t), \underline{\alpha}(t)) = \underline{e}_d(t)^\top M_{\partial} \underline{f}_{\partial}(t) - \underline{e}_d(t)^\top M_{\alpha} \underline{f}_d(t),$$

568 which contains the term $\underline{e}_d(t)^\top M_{\alpha} \underline{f}_d(t)$, non-negative if the dissipative con-
 569 stitutive relation $\mathcal{N}(h, \alpha, \underline{e}_d, \underline{f}_d) = 0$ is indeed a dissipation, *e.g.*, of the form
 570 $\underline{e}_d = C(\alpha, h) \underline{f}_d$, with $C(\alpha, h) \geq 0$. Such a constitutive relation would give
 571 at the discrete level: $M_{\alpha} \underline{e}_d = C[h^d, \alpha^d] \underline{f}_d$, with $C[h^d, \alpha^d] \geq 0$. In this latter
 572 case, the power balance becomes:

$$\begin{aligned} \frac{d}{dt} \mathcal{H}^d(\underline{h}(t), \underline{\alpha}(t)) &= \underline{e}_d(t)^\top M_{\partial} \underline{f}_{\partial}(t) - \underline{f}_d(t)^\top C[h^d(t), \alpha^d(t)] \underline{f}_d(t) \\ &\leq \underline{e}_d(t)^\top M_{\partial} \underline{f}_{\partial}(t). \end{aligned}$$

573 This encompasses the following empirical laws [81, § 7.2.6], which are
 574 used to model the friction of the fluid with the bottom of the channel:

- 575 • Fanning friction: $(C[h^d, \alpha^d])_{k,\ell} = C_f \int_{\Omega} \frac{\|\alpha^d\|}{h^d} \phi^\ell \cdot \phi^k \, d\Omega$;
- 576 • Manning friction: $(C[h^d, \alpha^d])_{k,\ell} = gn^2 \int_{\Omega} \frac{\|\alpha^d\|}{(h^d)^{\frac{4}{3}}} \phi^\ell \cdot \phi^k \, d\Omega$;
- 577 • Darcy-Weisbach: $(C[h^d, \alpha^d])_{k,\ell} = \frac{f_{DW}}{8} \int_{\Omega} \frac{\|\alpha^d\|}{h^d} \phi^\ell \cdot \phi^k \, d\Omega$;
- 578 • Kellerhals friction: $(C[h^d, \alpha^d])_{k,\ell} = gr^2 \int_{\Omega} \frac{\|\alpha^d\|}{(h^d)^{\frac{3}{2}}} \phi^\ell \cdot \phi^k \, d\Omega$.

579 *Linear dissipation of Navier-Stokes type.* Indeed, in addition to modeling the
 580 friction of the fluid with the bottom of the channel, viscous dissipation can
 581 be introduced by incorporating the analogue of the Navier-Stokes dissipative
 582 terms in the SWE model: it involves an unbounded linear operator. One
 583 could first guess to add a $-\Delta$ diffusion term, as was first proposed in [31];
 584 however the careful derivation of the damping model should be made with
 585 care, see [56] in 1D and [88] in 2D, where the model exhibits a h -dependent
 586 dissipation term. A structure-preserving pH discretization of this more ad-
 587 vanced model, involving symmetric tensors, can be found in [29].

588 *3.3. Example of the rotational SWE with boundary-feedback control*

589 In this example, previously discussed in [28], a boundary-feedback control
 590 law is used with the goal of damping the waves. Indeed, one of the moti-
 591 vations for using the pH framework is that applying passivity-based control
 592 laws is straightforward. For example, a simple boundary output-feedback as:

$$f_{\partial} = -ke_{\partial}, \quad (45)$$

593 leads (26) to the following power-balance:

$$\frac{d}{dt}\mathcal{H} = -k \int_{\partial\Omega} (e_{\partial})^2 d\gamma, \quad (46)$$

594 from which the Hamiltonian is monotonically decreasing $\frac{d}{dt}\mathcal{H} \leq 0$ if $k > 0$.

595 Recall that from (25), $e_{\partial} = -\mathbf{e}_{\alpha} \cdot \mathbf{n}$, is the ingoing volumetric fluid flux and
 596 $f_{\partial} = e_h$ is the pressure, both at the boundary.

597 This control law is of low applicability for the SWE, since it removes
 598 energy not only by damping the waves, but also by removing water from
 599 inside the tank (thus, the potential energy is reduced). For this reason, we
 600 used the following slightly modified control law:

$$f_{\partial} = -k(e_{\partial} - e_{\partial}^0), \quad (47)$$

601 where e_{∂}^0 is the desired output, given by the steady-state total pressure at
 602 the boundary ($e_h = \rho gh^0$) at the desired fluid height h^0 .

603 It is straightforward to prove that the previous boundary control law
 604 **stabilizes the infinite-dimensional dynamical system in the sense of Lyapunov**
 605 **around an equilibrium**: We can define a “desired Hamiltonian”, or Lyapunov
 606 function, given by:

$$V = \int_{\Omega} \left[\frac{1}{2} \rho g (h - h^0)^2 + \frac{1}{2\rho} h \|\boldsymbol{\alpha}\|^2 \right] d\Omega, \quad (48)$$

607 By computing the time-derivative of the Lyapunov function along trajecto-
 608 ries, using the feedback law proposed in (47), we get:

$$\dot{V} = -k \int_{\partial\Omega} (e_{\partial} - e_{\partial}^0(\theta))^2 d\gamma. \quad (49)$$

609 Thus, if $k > 0$, the Lyapunov function shall reduce monotonically towards
 610 the minimum point of (48) ($h = h^0$ and $\boldsymbol{\alpha} = \mathbf{0}$).

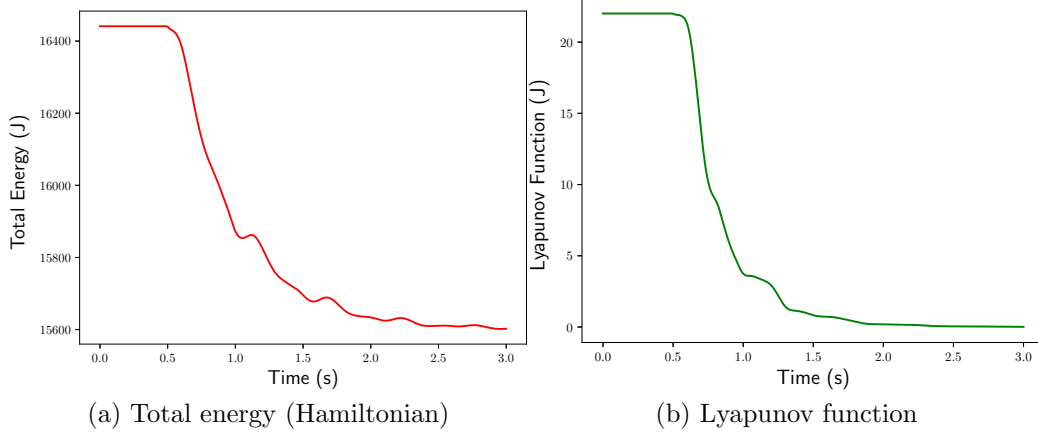


Figure 2: Total energy and Lyapunov Function

611 *Numerical results for the closed-loop SWE*

612 The feedback control law, from (47), can be implemented as an additional
 613 constitutive relationship that relates \underline{f}_∂ and \underline{e}_∂ in the finite-dimensional ap-
 614 proximated system (41).

615 The following simulation considers a circular tank with radius R , with
 616 radial coordinate r and polar coordinate θ , assuming the following initial
 617 conditions:

$$\begin{aligned} h(t = 0, r, \theta) &= \cos(\pi r/R) \cos(2\theta), \\ \boldsymbol{\alpha}(t = 0, r, \theta) &= \rho \mathbf{u} = \mathbf{0}. \end{aligned} \quad (50)$$

618 The boundary conditions are assumed to be:

$$\begin{aligned} f_\partial &= 0, t \leq 0.5s, \\ f_\partial &= -k (e_\partial(t, s) - e_\partial^0), t > 0.5s, \end{aligned} \quad (51)$$

619 *i.e.* the feedback control law proposed is activated after 0.5s of simulation.
 620 A video of this simulation can be downloaded in <https://nextcloud.isae.fr/index.php/s/4TrMBSZa86cL6w2>.
 621

622 Continuous Galerkin elements with 1st-order Lagrange polynomials are
 623 used for approximating the h variable, and discontinuous Galerkin elements
 624 with 0-order Lagrange polynomials are used for approximating the $\boldsymbol{\alpha}$ vari-
 625 ables. The system Hamiltonian as well as the Lyapunov function are pre-
 626 sented as a function of time in Fig. 2. Note that during the first 0.5 s of the

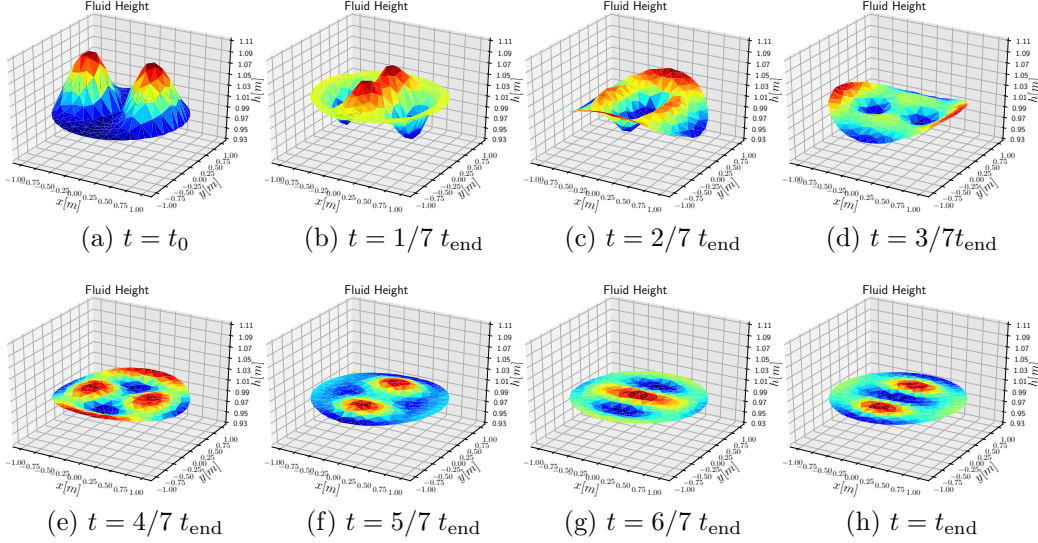


Figure 3: Boundary control using a proportional gain $t_{\text{end}} = 3[s]$

627 simulation, both the Hamiltonian (total energy) and the Lyapunov function
 628 are constant. After 0.5 s, the Hamiltonian reduces and oscillates until con-
 629 verging to the new energy minimum. The Lyapunov function monotonically
 630 decreases towards zero. Snapshots of the simulation are presented in Fig. 3.

631 3.4. Example of the incompressible Navier-Stokes equations

632 In order to reduce as much as possible the number of degrees of freedom
 633 needed to discretize the incompressible NSE in a structure-preserving way,
 634 the vorticity–stream function formulation has been chosen in Section 2.4.
 635 However, some adaptations are required for the boundary controls to remain
 636 identical to those of the initial system, as another term appears in the power
 637 balance (37). Furthermore, the constitutive relation linking the vorticity ω
 638 to the stream function ψ reveals differential: $-\Delta\psi = \omega$. This means that at
 639 least two choices are possible for the resolution in time of the discrete system:
 640 either we differentiate twice, requiring sufficiently rich finite elements, or we
 641 perform an integration by part to reduce the order of derivation, to the price
 642 of another boundary term, involving the time derivative of the control. In the
 643 following, the latter is chosen, in an implicit form: the constitutive relation
 644 is embedded in the dynamical system, see (52).

645 Indeed, to reduce the complexity of the system, an efficient strategy is to

646 consider the *co-energy formulation*, involving only the co-energy and effort
 647 variables by substituting the constitutive relations into the dynamical system:
 648 $-\Delta\psi = \omega$, and $\mu_c^{-1} e_c = f_c$ are used in (36), leading to the system:

$$\begin{pmatrix} -\rho_0 \Delta\partial_t\psi \\ \mu_c^{-1} e_c \end{pmatrix} = \begin{bmatrix} J_\omega & -\text{curl}_{2D} \mathbf{grad}^\perp \\ \text{curl}_{2D} \mathbf{grad}^\perp & 0 \end{bmatrix} \begin{pmatrix} \psi \\ e_c \end{pmatrix}. \quad (52)$$

649 We may now apply the PFEM: we write the weak formulation of (52), per-
 650 form appropriate integration by part, and project the system on finite element
 651 families.

652 For all sufficiently smooth test functions (φ, Φ) , one has:

$$\begin{cases} -\int_{\Omega} \rho_0 \partial_t \Delta\psi \varphi \, d\Omega = \int_{\Omega} J_\omega \psi \varphi \, d\Omega - \int_{\Omega} \text{curl}_{2D} \mathbf{grad}^\perp(e_c) \varphi \, d\Omega, \\ \int_{\Omega} \mu_c^{-1} e_c \Phi \, d\Omega = \int_{\Omega} \text{curl}_{2D} \mathbf{grad}^\perp(\psi) \Phi \, d\Omega. \end{cases} \quad (53)$$

653 Every differential operators in this system, including J_ω , are of second order.
 654 Let us integrate by part on each of them.

$$\begin{aligned} & -\int_{\Omega} \rho_0 \partial_t \Delta\psi \varphi \, d\Omega = -\int_{\Omega} \rho_0 \Delta\partial_t\psi \varphi \, d\Omega \\ & = \int_{\Omega} \rho_0 \mathbf{grad}(\partial_t\psi) \cdot \mathbf{grad}(\varphi) \, d\Omega - \int_{\partial\Omega} \rho_0 \mathbf{grad}(\partial_t\psi) \cdot \mathbf{n} \varphi \, d\gamma \quad (54) \\ & = \int_{\Omega} \rho_0 \mathbf{grad}(\partial_t\psi) \cdot \mathbf{grad}(\varphi) \, d\Omega - \int_{\partial\Omega} \rho_0 \partial_t \underbrace{\mathbf{grad}(\psi) \cdot \mathbf{n}}_{\mathbf{u} \wedge \mathbf{n} = u_\tau} \varphi \, d\gamma. \end{aligned}$$

655

$$\begin{aligned} \int_{\Omega} J_\omega \psi \varphi \, d\Omega & = \int_{\Omega} \text{div}(\omega \mathbf{grad}^\perp(\psi)) \varphi \, d\Omega \\ & = -\int_{\Omega} \omega \mathbf{grad}^\perp(\psi) \cdot \mathbf{grad}(\varphi) \, d\Omega \quad (55) \\ & \quad + \int_{\partial\Omega} \omega \underbrace{\mathbf{grad}^\perp(\psi) \cdot \mathbf{n}}_{\mathbf{u} \cdot \mathbf{n} = u_n} \varphi \, d\gamma. \end{aligned}$$

656

$$\begin{aligned} -\int_{\Omega} \text{curl}_{2D} \mathbf{grad}^\perp(e_c) \varphi \, d\Omega & = -\int_{\Omega} \mathbf{grad}^\perp(e_c) \cdot \mathbf{grad}^\perp(\varphi) \, d\Omega \\ & \quad + \int_{\partial\Omega} \underbrace{(\mathbf{grad}(e_c)) \cdot \mathbf{n}}_{=y_c} \varphi \, d\gamma. \end{aligned} \quad (56)$$

670 $i \in \{1, \dots, N_\psi\}$ and $\Phi = \Phi^k$ for all $k \in \{1, \dots, N_c\}$ as test functions:

$$\begin{bmatrix} M_\psi & 0 \\ 0 & M_c \end{bmatrix} \begin{pmatrix} \underline{\dot{\psi}} \\ \underline{e_c} \end{pmatrix} = \begin{bmatrix} J_\omega[\omega^d] & -D \\ D^\top & 0 \end{bmatrix} \begin{pmatrix} \underline{\psi} \\ \underline{e_c} \end{pmatrix} + \begin{bmatrix} B_n[\omega^d] & 0 & B_{dt} & B_c \\ 0 & B_\tau & 0 & 0 \end{bmatrix} \begin{pmatrix} \underline{u_n} \\ \underline{u_\tau} \\ \underline{\dot{u}_\tau} \\ \underline{y_c} \end{pmatrix}, \quad (59)$$

where $\underline{\square}$ is the collection of the time-dependent coefficients of the approximation \square^d in the associated finite element basis, and:

$$\begin{aligned} (M_\psi)_{i,j} &:= \int_\Omega \rho_0 \mathbf{grad}(\varphi^j) \cdot \mathbf{grad}(\varphi^i) \, d\Omega, & (M_c)_{k,\ell} &:= \int_\Omega \mu_c^{-1} \Phi^\ell \Phi^k \, d\Omega, \\ (J_\omega[\omega^d])_{i,j} &:= \int_\Omega \omega^d \mathbf{grad}^\perp(\varphi^j) \cdot \mathbf{grad}(\varphi^i) \, d\Omega, \\ (D)_{i,\ell} &:= \int_\Omega \mathbf{grad}^\perp(\Phi^\ell) \cdot \mathbf{grad}^\perp(\varphi^i) \, d\Omega, \\ (B_n[\omega^d])_{i,n} &:= \int_{\partial\Omega} \omega^d \xi^n \varphi^i \, d\gamma, & (B_\tau)_{k,n} &:= - \int_{\partial\Omega} \xi^n \Phi^k \, d\gamma, \\ (B_{dt})_{k,n} &:= \int_{\partial\Omega} \rho_0 \xi^n \varphi^i \, d\gamma, & (B_c)_{i,n} &:= \int_{\partial\Omega} \xi^n \varphi^i \, d\gamma. \end{aligned}$$

671 Note that $D \in \mathbb{R}^{N_\psi \times N_c}$ is not square in general (as $B_n[\omega^d], B_c, B_{dt} \in \mathbb{R}^{N_\psi \times N_\partial}$
672 and $B_\tau \in \mathbb{R}^{N_c \times N_\partial}$).

673 **Remark 13.** *Interestingly, integration by parts has been here performed on*
674 *both lines, while PFEM usually relies on one integration by parts on the*
675 *appropriate line (depending on the considered causality).*

Dirac-structure and power balance. Let us consider the colocated boundary observations $\underline{y_n}$, $\underline{y_\tau}$ and $\underline{y_{dt}}$ as well as the colocated control $\underline{u_c}$, obtained by taking the transpose of the big control matrix on the right-hand side of (59):

$$\begin{bmatrix} M_\partial & 0 & 0 & 0 \\ 0 & M_\partial & 0 & 0 \\ 0 & 0 & M_\partial & 0 \\ 0 & 0 & 0 & M_\partial \end{bmatrix} \begin{pmatrix} \underline{y_n} \\ \underline{y_\tau} \\ \underline{y_{dt}} \\ \underline{u_c} \end{pmatrix} = \begin{bmatrix} B_n[\omega^d]^\top & 0 \\ 0 & B_\tau^\top \\ B_{dt}^\top & 0 \\ B_c^\top & 0 \end{bmatrix} \begin{pmatrix} \underline{\psi} \\ \underline{e_c} \end{pmatrix},$$

where:

$$(M_\partial)_{m,\ell} := \int_{\partial\Omega} \xi^\ell \xi^m \, d\gamma,$$

676 is the boundary mass matrix.

677 Then, a discrete Dirac structure is given by gathering the above and (59)
678 as follows:

$$\underbrace{\text{Diag} \begin{bmatrix} M_\psi \\ M_c \\ M_\partial \\ M_\partial \\ M_\partial \\ M_\partial \end{bmatrix}}_{\mathbf{M}} \begin{pmatrix} \dot{\underline{\psi}} \\ \underline{e}_c \\ -\underline{y}_n \\ -\underline{y}_\tau \\ -\underline{y}_{dt} \\ \underline{u}_c \end{pmatrix} = \underbrace{\begin{bmatrix} J_\omega[\omega^d] & -D & B_n[\omega^d] & 0 & B_{dt} & -B_c \\ D^\top & 0 & 0 & B_\tau & 0 & 0 \\ -B_n[\omega^d]^\top & 0 & 0 & 0 & 0 & 0 \\ 0 & -B_\tau^\top & 0 & 0 & 0 & 0 \\ -B_{dt}^\top & 0 & 0 & 0 & 0 & 0 \\ B_c^\top & 0 & 0 & 0 & 0 & 0 \end{bmatrix}}_{\mathbf{J}} \begin{pmatrix} \underline{\psi} \\ \underline{e}_c \\ \underline{u}_n \\ \underline{u}_\tau \\ \dot{\underline{u}}_\tau \\ -\underline{y}_c \end{pmatrix}. \quad (60)$$

679 This Dirac structure will help computing the power balance satisfied by the
680 discrete Hamiltonian, defined as the continuous one (35) evaluated in the
681 discretization of the energy variable ω^d . Two difficulties arise: first, we recall
682 that ω is implicit in the definition (35), second, we do not have access to $\underline{\omega}$
683 in our simulation, but to $\underline{\psi}$ and \underline{e}_c . Nevertheless, the following proposition
684 holds true.

685 **Proposition 9.** *The discrete Hamiltonian can be defined as:*

$$\begin{aligned} \mathcal{H}^d(\underline{\omega}) &= \frac{1}{2} \int_{\Omega} \rho_0 \|\mathbf{grad}(\psi^d)\|^2 d\Omega, \\ &= \frac{1}{2} \underline{\psi}^\top M_\psi \underline{\psi}. \end{aligned} \quad (61)$$

Proof. By definition of the stream function ψ , one has $\mathbf{u} = \mathbf{grad}^\perp(\psi)$. At
the discrete level, this reads $\mathbf{u}^d = \mathbf{grad}^\perp(\psi^d)$, hence:

$$\mathcal{H}^d(\underline{\omega}) = \frac{1}{2} \int_{\Omega} \rho_0 \|\mathbf{grad}^\perp(\psi^d)\|^2 d\Omega,$$

686 holds. Furthermore, a trivial computation shows that $\|\mathbf{grad}^\perp(\psi^d)\|^2 =$
687 $\|\mathbf{grad}(\psi^d)\|^2$, leading to the first claimed equality. Replacing $\psi^d(\boldsymbol{\zeta}, t)$ by
688 the sum $\sum_{i=1}^{N_\psi} \psi^i(t) \varphi^i(\boldsymbol{\zeta})$ gives the second claimed equality. \square

689 **Remark 14.** *The discretization \mathbf{u}^d of the velocity field as defined above is*
690 *consistent with both the discrete stream function ψ^d (by definition) and the*
691 *discrete vorticity ω^d . Indeed, ω^d must satisfy $\omega^d = \text{curl}_{2D} \mathbf{u}^d$, which becomes*
692 *$\omega^d = \text{curl}_{2D} \mathbf{grad}^\perp(\psi^d) = -\Delta \psi^d$ (in a weak sense), i.e. the constitutive*
693 *relation that has been used to eliminate ω^d .*

Remark 15. The “mass” matrix M_ψ is a stiffness-like matrix in this particular case where the constitutive relation $-\Delta\psi = \omega$ has been embedded into the dynamical system. It is not positive-definite, however, the big block diagonal “mass” matrix \mathbf{M} on the left-hand side of the Dirac structure (60) is positive-definite as soon as the initial value of the boundary control $\underline{u}_c(0)$ is compatible with the initial value of $\underline{\phi}(0)$, i.e., on:

$$X := \left\{ \left(\underline{\psi}^\top \quad \underline{e}_c^\top \quad -\underline{y}_n^\top \quad -\underline{y}_\tau^\top \quad -\underline{y}_{dt}^\top \quad \underline{u}_c^\top \right)^\top \in \mathbb{R}^{N_\psi + N_c + 4N_\partial} \mid B_c^\top \underline{\psi} = M_\partial \underline{u}_c \right\},$$

as a subspace of $\mathbb{R}^{N_\psi + N_c + 4N_\partial}$. Indeed, one has a symmetric positive matrix. Assume that $\left(\underline{\psi}^\top \quad \underline{e}_c^\top \quad -\underline{y}_n^\top \quad -\underline{y}_\tau^\top \quad -\underline{y}_{dt}^\top \quad \underline{u}_c^\top \right)^\top \in \text{Ker} \mathbf{M} \subset X$, then $M_\psi \underline{\psi} = 0$. Now, recall that:

$$(M_\psi)_{i,j} := \int_{\Omega} \rho_0 \mathbf{grad}(\varphi^j) \cdot \mathbf{grad}(\varphi^i) \, d\Omega,$$

694 hence, $M_\psi \underline{\psi} = 0$ implies that ψ^d is constant (and the associated velocity field
 695 \mathbf{u}^d is null). Since on the kernel, $M_\partial \underline{u}_c = 0$, one has $B_c^\top \underline{\psi} = 0$ in X . Or in
 696 other words: the Dirichlet trace of $\underline{\psi}^d$ is identically zero, implying that the
 697 constant approximated function ψ^d is identically zero. Finally, this proves
 698 that $\text{Ker} \mathbf{M} = \{0\}$ on X , hence \mathbf{M} is positive-definite.

699 With Proposition 9 and the discrete Dirac structure (60) at hand, the
 700 power balance can be computed.

701 **Theorem 10.** Let $(\underline{\psi}, \underline{e}_c, \underline{y}_n, \underline{y}_\tau, \underline{y}_{dt}, \underline{y}_c)$ be a trajectory, i.e., a solution to (60)
 702 for some initial data and compatible controls $\underline{u}_n \in C^0(0, \infty; \mathbb{R}^{N_\partial})$, $\underline{u}_\tau \in$
 703 $C^1(0, \infty; \mathbb{R}^{N_\partial})$ and $\underline{u}_c \in C^0(0, \infty; \mathbb{R}^{N_\partial})$. Then the following power balance
 704 holds true for $t \geq 0$:

$$\frac{d}{dt} \mathcal{H}^d(\underline{\omega}) = -\underline{e}_c^\top M_c \underline{e}_c + \underline{u}_n^\top M_\partial \underline{y}_n + \underline{u}_\tau^\top M_\partial \underline{y}_\tau + \underline{y}_c^\top M_\partial \underline{u}_c, \quad (62)$$

705 which preserves the power balance (37) at the discrete level.

706 *Proof.* See Appendix B.4 □

707 *Numerical results for the lid-driven cavity problem*

708 The vorticity-stream function formulation allows for the simulation to be
 709 done at a reduced cost. To test its precision, let us consider the lid-driven

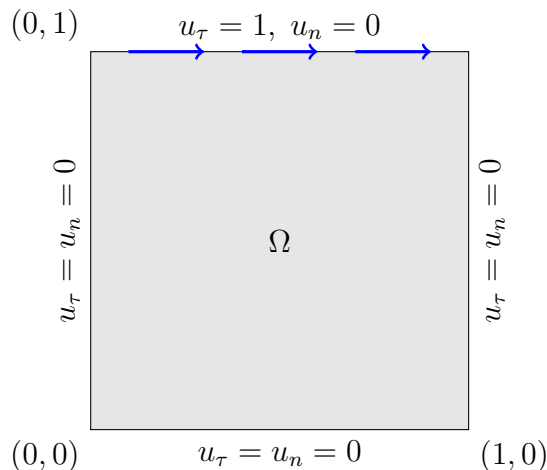


Figure 4: The configuration of the lid-driven cavity test case.

710 cavity problem, for which benchmarks can be found at the following address:
 711 <http://www.zetacomp.com>, and are addressed in [58].

712 The lid-driven cavity problem is a particular 2D test case where the fluid
 713 fills a unit square and is controlled tangentially by the upper boundary of
 714 the square at a constant velocity of 1 m.s^{-1} , see Figure 4.

715 In the sequel, the simulations are performed in python, using GMSH [57]
 716 as mesh generator, FEniCS [85] as finite element library and PETSc [1] for
 717 the time integration of the resulting nonlinear DAE. The meshes are refined
 718 near the upper corners of the square, as the highest velocity variations (hence,
 719 values for the vorticity), will occur at these spots. In all the simulations, the
 720 initial data are identically null, and the boundary control is constant and
 721 applied as soon as $t > 0$. Videos of these simulations can be downloaded in
 722 <https://nextcloud.isae.fr/index.php/s/4TrMBSZa86cL6w2>.

723 *Reynolds 100.* The first simulations are done at Reynolds 100, *i.e.*, for a fluid
 724 of mass density $\rho_0 \equiv 1$, with a viscosity $\mu = 1.e^{-2}$. At this Reynolds number,
 725 one vortex takes place in the square.

726 The finite element families are chosen as follows: continuous Lagrange
 727 finite elements of order 2 \mathbb{P}^2 for the co-energy variable ψ , continuous La-
 728 grange finite elements of order 1 \mathbb{P}^1 for the effort variable e_c , and boundary
 729 continuous Lagrange finite elements of order 1 \mathbb{P}^1 for all boundary fields.

730 The discretization of the square leads to about 10,000 degrees of freedom.
 731 One may appreciate how the streamlines are recovered when the dynamical

732 system reaches the stationary solution, as can be observed in Figure 5.

733 *Reynolds 400.* The viscosity is lowered at $\mu = 2.5e^{-3}$. At this Reynolds
734 number, a first recirculation area appears in the lower-right corner of the
735 square.

736 The finite element families are chosen as for the case $\mu = 1.e^{-2}$.

737 The simulation requires a finer discretization of the domain to capture
738 the higher variations of velocity in the fluid, which leads to 40,000 degrees of
739 freedom. Figure 6 shows the development of the two vortices, and how the
740 chosen strategy allows recovering the evolution to the stationary solution.

741 *Reynolds 1000.* Now, the viscosity is $\mu = 1.e^{-3}$. At this Reynolds number, a
742 second recirculation area appears in the lower-left corner of the square.

743 The finite elements families are chosen as follows: continuous Lagrange
744 finite elements of order 3 \mathbb{P}^3 for the co-energy variable ψ , continuous La-
745 grange finite elements of order 2 \mathbb{P}^2 for the effort variable e_c , and boundary
746 continuous Lagrange finite elements of order 1 \mathbb{P}^1 for all boundary fields.

747 The discretization is again finer than previously, once more, to consider
748 higher variations in the velocity field. To improve the numerical behavior
749 near the first recirculation area, the lower-right corner is also refined. These
750 refinements and higher orders of finite elements lead to a nonlinear DAE of
751 size 360,000. One may see in Figure 7 the efficiency of the proposed approach:
752 both recirculation areas are captured, and the center of the main vortex is
753 well-recovered.

754 **Remark 16.** *Discretizing the velocity–vorticity–pressure formulation (31)*
755 *would have required about one million degrees of freedom to reach the same*
756 *precision (even after substitution of the constitutive relation $e_c = \mu_c \mathbf{f}_c$ into (31),*
757 *as $\mathbf{f}_c = \mu_c^{-1} e_c$). In this 2D setting, the computational burden has been signif-*
758 *icantly reduced by using the vorticity–stream function formulation (52), while*
759 *preserving the underlying geometric structure of the physical phenomena at*
760 *the discrete level.*

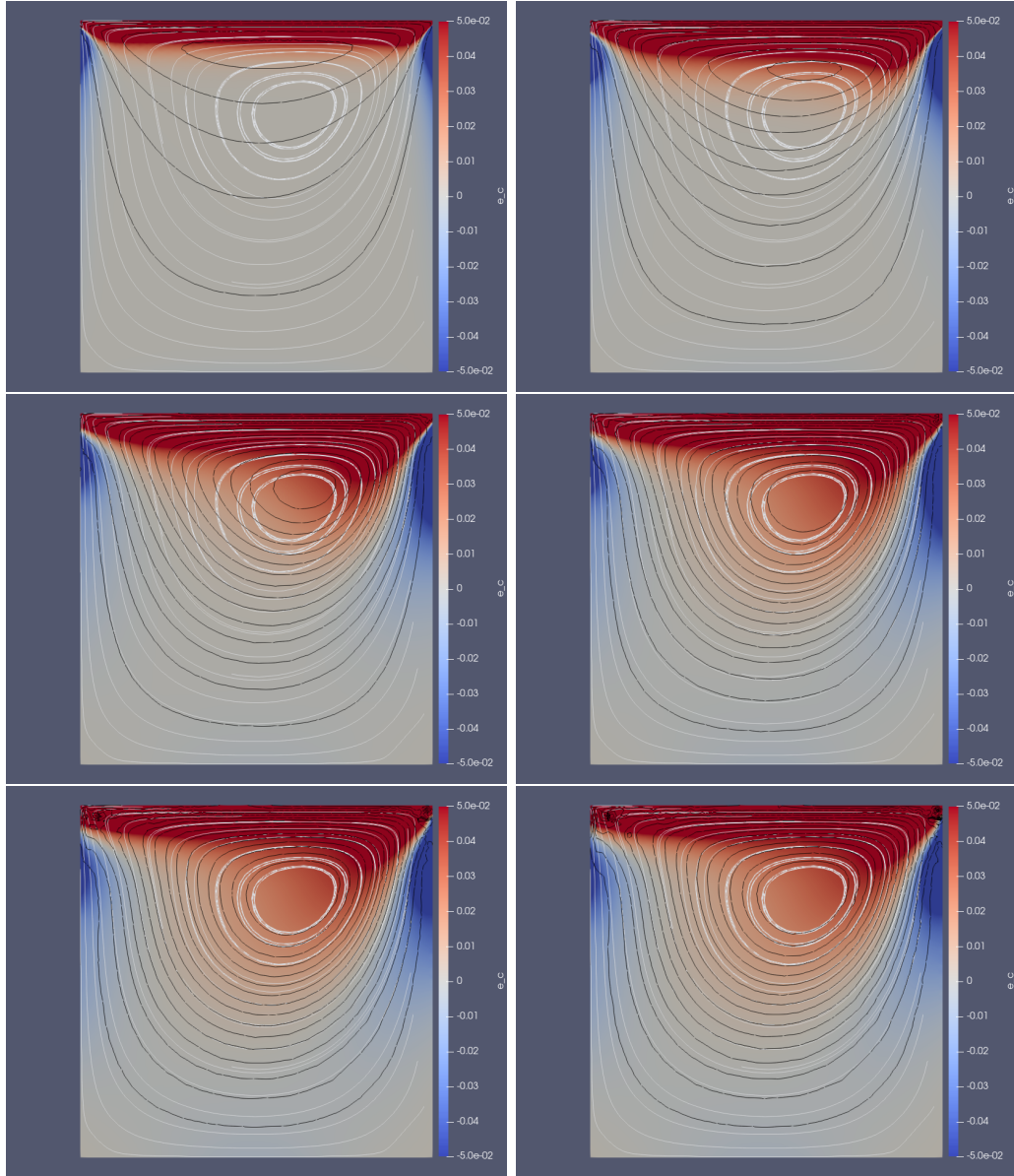


Figure 5: Lid-driven cavity problem at Reynolds 100 ($\mu = 1.e^{-2}$) at times $t = 0.1, 0.5, 2, 4, 8,$ and 10 s. The color represents the effort variable $e_c = \mu\omega$, while the solid black lines are streamlines, to compare with the white streamlines from [58].

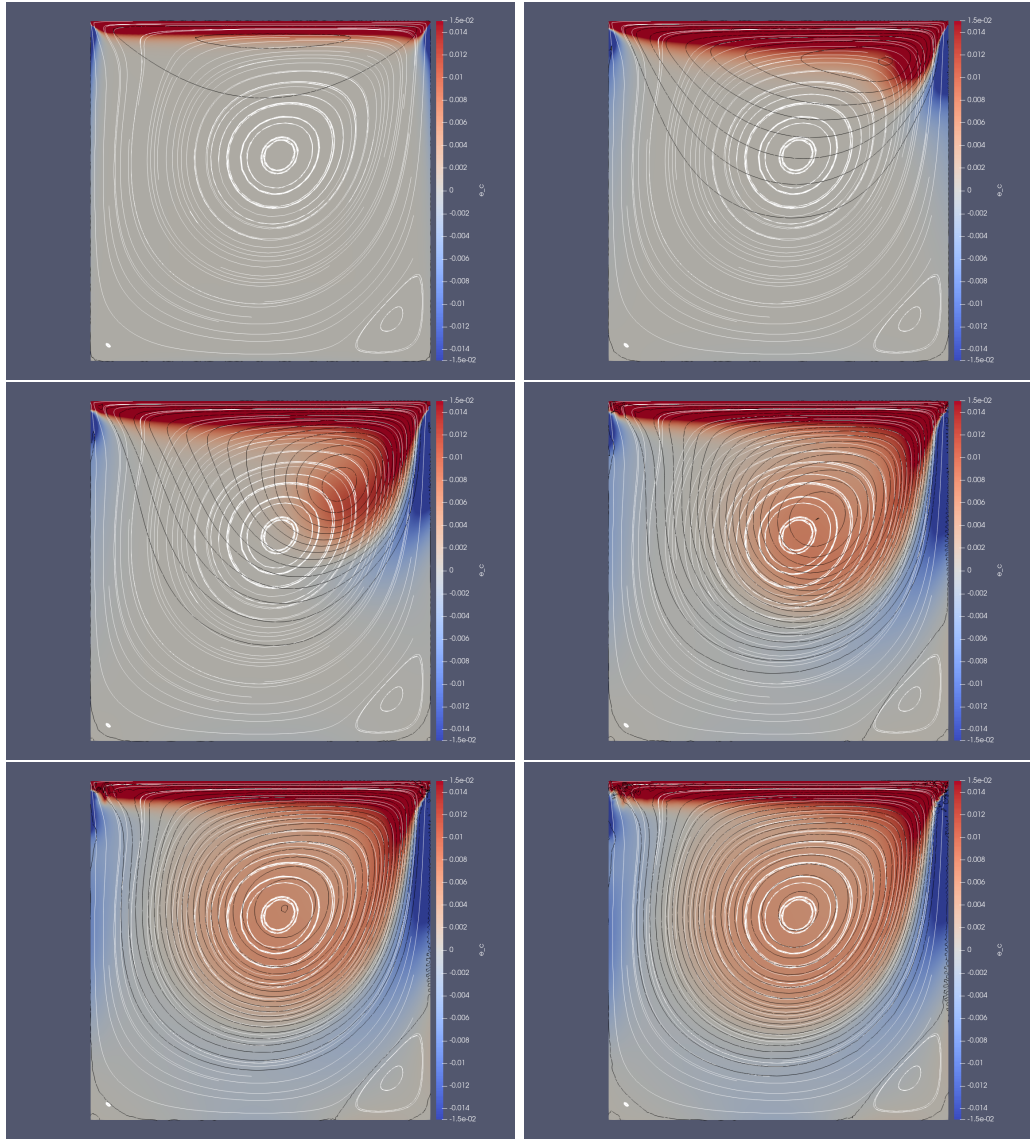


Figure 6: Lid-driven cavity problem at Reynolds 400 ($\mu = 2.5e^{-3}$) at times $t = 0.1, 1, 3, 7, 12,$ and 18 s. The color represents the effort variable $e_c = \mu\omega$, while the solid black lines are streamlines, to compare with the white streamlines from [58].

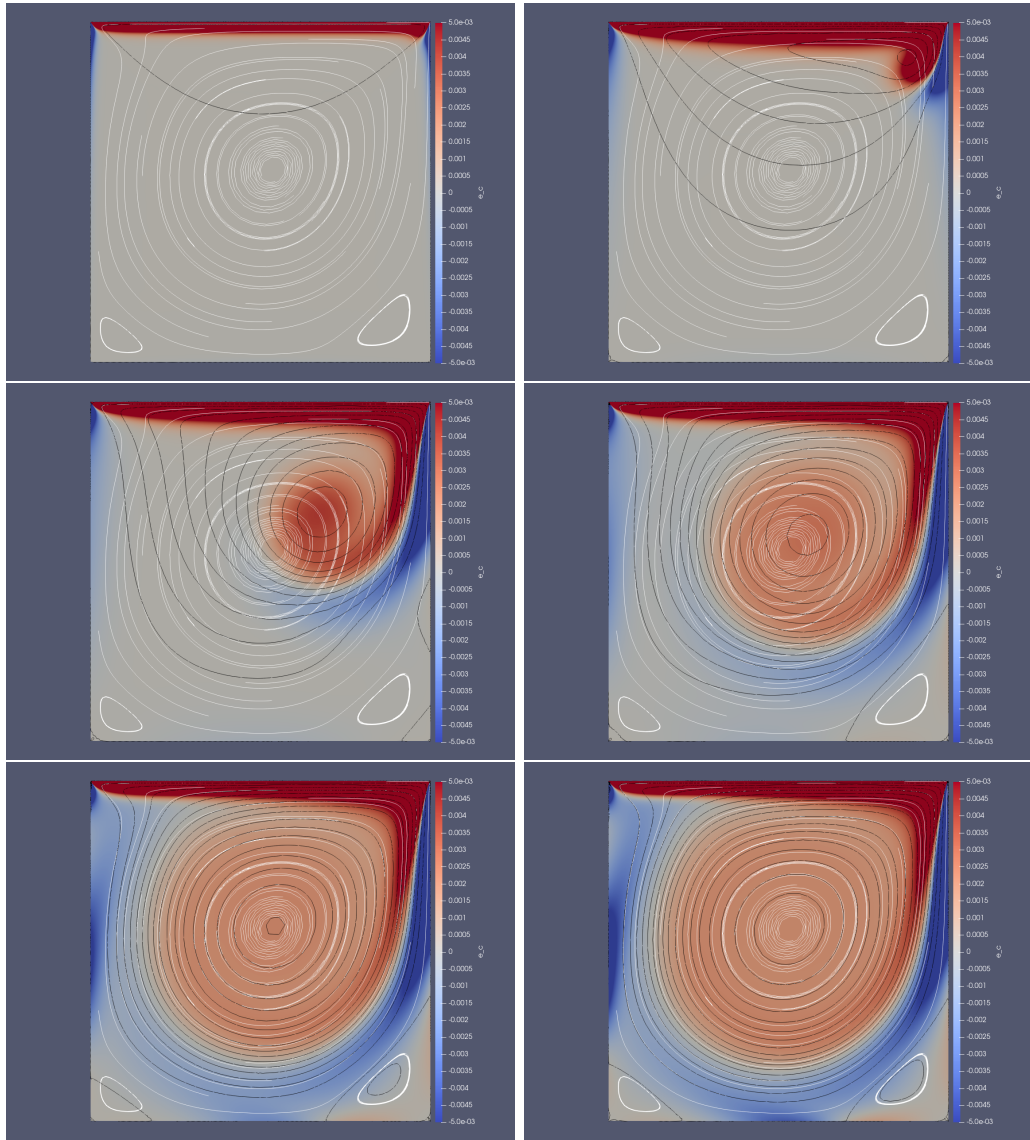


Figure 7: Lid-driven cavity problem at Reynolds 1000 ($\mu = 1.e^{-3}$) at times $t = 0.1, 1, 5, 10, 18,$ and 35 s. The color represents the effort variable $e_c = \mu\omega$, while the solid black lines are streamlines, to compare with the white streamlines from [58].

761 4. Extension to thermodynamics

762 If thermal phenomena cannot be neglected then the thermal domain needs
 763 to be taken into account in the model. This Section focuses on Irreversible

764 pH (IpH) systems, which is a **specific** thermodynamic formulation closely
765 related to dissipative pH systems. It is shown how by relating the dissipa-
766 tive ports of a pH system with the *entropy production* a quasi pH structure
767 arises which assures both energy conservation and irreversible entropy cre-
768 ation. Furthermore, by introducing a class of pseudo-bracket it is possible to
769 precisely parametrize the quasi pH structure by the thermodynamic driving
770 forces which induce the irreversible phenomena in the system. The develop-
771 ments are illustrated by systematically developing the 1D SWE.

772 4.1. Quasi pH system

Recall the formulation of dissipative pH systems which are of the form
 $\partial_t \mathbf{x}(\boldsymbol{\zeta}, t) = \mathcal{J} \delta_{\mathbf{x}} \mathcal{H} - \mathcal{G} S \mathcal{G}^* \delta_{\mathbf{x}} \mathcal{H}$, where \mathcal{G} is a differential operator and \mathcal{G}^*
the corresponding formal adjoint, and $S \geq 0$ is a non-negative bounded
matrix operator of appropriate dimensions. In this case, $\mathcal{G} S \mathcal{G}^*$ represents
the dissipation and can be split into two parts such to express the dissipative
pH system from an extended Dirac structure as

$$\begin{pmatrix} \partial_t \mathbf{x}(\boldsymbol{\zeta}, t) \\ \mathbf{f}_d \end{pmatrix} = \underbrace{\begin{bmatrix} \mathcal{J} & \mathcal{G} \\ -\mathcal{G}^* & 0 \end{bmatrix}}_{\tilde{\mathcal{J}}} \begin{pmatrix} \mathbf{e} \\ \mathbf{e}_d \end{pmatrix}, \quad \text{with } \mathbf{e}_d = S \mathbf{f}_d, \quad (63)$$

$$\begin{pmatrix} \mathbf{f}_\partial \\ \mathbf{e}_\partial \end{pmatrix} = \tilde{\mathcal{W}}_{\partial\Omega} \begin{pmatrix} \mathbf{e}|_{\partial\Omega} \\ \mathbf{e}_d|_{\partial\Omega} \end{pmatrix}, \quad (64)$$

where $\partial_t \mathbf{x}(\boldsymbol{\zeta}, t) \in \mathcal{F}$ and $S > 0$. $\tilde{\mathcal{J}}$ is an extended formally skew-symmetric
differential operator, \mathbf{f}_∂ and \mathbf{e}_∂ are the boundary flow and effort port vari-
ables, $\tilde{\mathcal{W}}_{\partial\Omega}$ is an operator dependent on the unitary vector \mathbf{n} outward to $\partial\Omega$,
that describes the normal and tangential projections on $\partial\Omega$, induced by $\tilde{\mathcal{J}}$,
of the co-energy variables $\mathbf{e} := \delta_{\mathbf{x}} \mathcal{H}$ and dissipative effort \mathbf{e}_d , such that,

$$\dot{\mathcal{H}} = \int_{\partial\Omega} \mathbf{f}_\partial \cdot \mathbf{e}_\partial \, d\gamma - \int_{\Omega} \mathbf{f}_d \cdot \mathbf{e}_d \, d\Omega, \quad (65)$$

773 where $\int_{\partial\Omega} \mathbf{f}_\partial \cdot \mathbf{e}_\partial \, d\gamma$ describes the power supplied to the system through the
774 boundaries and $\int_{\Omega} \mathbf{f}_d \cdot \mathbf{e}_d \, d\Omega$ the power dissipated into heat by the internal
775 phenomena (such as friction or viscosity). As discussed in subsection 2.2,
776 the formulation (63) is very convenient for numerical approximations [91],
777 since the extended operator $\tilde{\mathcal{J}}$ is linear. However, the resolution of the
778 system dynamics is implicit since the dissipative port introduce an algebraic
779 constraint.

780 In the case of the dissipative SWE example, the formulation (63) is of the
 781 form

$$\begin{pmatrix} \partial_t q \\ \partial_t \alpha \\ f_d \end{pmatrix} = \begin{pmatrix} 0 & -\partial_\zeta & 0 \\ -\partial_\zeta & 0 & 1 \\ 0 & -1 & 0 \end{pmatrix} \begin{pmatrix} e_q \\ e_\alpha \\ e_d \end{pmatrix}, \quad (66)$$

with $e_d = S f_d$ and with power balance given by

$$\dot{\mathcal{H}} = - \int_{[0,L]} S f_d^2 d\zeta + \mathbf{e}_\partial^T \mathbf{f}_\partial = - \int_{[0,L]} S e_\alpha^2 d\zeta + \mathbf{e}_\partial^T \mathbf{f}_\partial, \quad (67)$$

782 where $\mathcal{G} = [0 \ 1]^T$ and $S = S(q, \alpha) \geq 0$ is a nonlinear function of the energy
 783 variables q and α .

784 Regarding the general formulation (63), if $\mathcal{G} = 0$, then the boundary
 785 controlled system is energy preserving or reversible. If $\mathcal{G} \neq 0$ the system
 786 is dissipative, meaning that energy is being transformed into heat by some
 787 dissipative phenomena, such as mechanical friction. Note that these implicit
 788 formulations have been recently extended to pH systems formulations defined
 789 on Lagrange submanifolds, to cope with a larger class of systems involving
 790 an implicit definition of the energy [123, 122].

791 An alternative approach consists in representing explicitly the thermal
 792 domain in the system formulation using the entropy density variable s and
 793 the total energy [121], preferably to the mechanical, electrical or magnetic
 794 energies. In this case, the total energy of the system can be split as the sum
 795 of the mechanical, electrical or magnetic energy (or the sum of them) and
 796 the internal energy $\int_{[0,L]} e(s) d\zeta$:

$$H(\mathbf{x}, s) = \mathcal{H}(\mathbf{x}) + \int_{[0,L]} e(s) d\zeta,$$

where s is the entropy per unit length. From the first law, in the absence of
 exchange of energy with the surroundings, i.e. $\mathbf{e}_\partial \mathbf{f}_\partial = 0$, the total energy is
 preserved, implying:

$$\begin{aligned} \dot{H} &= \dot{\mathcal{H}} + \int_{[0,L]} \dot{e}(s) d\zeta = 0, \\ &= \int_{[0,L]} (-f_d e_d + \partial_s e \partial_t s) d\zeta = 0, \\ &= \int_{[0,L]} (-\delta_{\mathbf{x}} \mathcal{H} (\mathcal{G} S \mathcal{G}^*) \delta_{\mathbf{x}} \mathcal{H} + \partial_s e \partial_t s) d\zeta = 0. \end{aligned}$$

Noticing that $\delta_{\mathbf{x}}\mathcal{H} = \delta_{\mathbf{x}}H$ and recalling from Gibbs' fundamental relation that the temperature is a function of the entropy, in this case $T = \partial_s e$, the internal entropy creation density, σ , of the system is explicitly written as:

$$\partial_t s = \frac{1}{T} \delta_{\mathbf{x}} H^T (\mathcal{G} S \mathcal{G}^*) \delta_{\mathbf{x}} H = \sigma \geq 0,$$

797 in accordance with the second law of Thermodynamics. The resulting system
798 is then:

$$\begin{bmatrix} \partial_t \mathbf{x} \\ \partial_t s \end{bmatrix} = \begin{bmatrix} \mathcal{J} & -(\mathcal{G} S \mathcal{G}^*) \delta_{\mathbf{x}} \mathcal{H} \frac{1}{T} \\ \frac{1}{T} \delta_{\mathbf{x}} H^T (\mathcal{G} S \mathcal{G}^*)^* & 0 \end{bmatrix} \begin{bmatrix} \delta_{\mathbf{x}} H \\ T \end{bmatrix}, \quad (68)$$

799 which corresponds to a quasi pH system [115], since it resembles a pH system,
800 but its structure matrix operator is a function of the gradient of the energy.
801 The formulation (68) allows to explicitly solve the dynamic equations of
802 the system. However, the symplectic structure of the pH system, given by
803 the Poisson tensor associated with the structure matrix, is now destroyed,
804 and the structure matrix is no longer linear; hence the numerical schemes
805 discussed in previous sections need to be rethought. In order to illustrate
806 this new formulation with a concrete example, consider again the dissipative
807 1D SWE of § 2.3.1. Its quasi pH system formulation is:

$$\begin{pmatrix} \partial_t q \\ \partial_t \alpha \\ \partial_t s \end{pmatrix} = \begin{pmatrix} 0 & -\partial_\zeta & 0 \\ -\partial_\zeta & 0 & -\frac{S}{T} e_\alpha \\ 0 & \frac{S}{T} e_\alpha & 0 \end{pmatrix} \begin{pmatrix} e_q \\ e_\alpha \\ T \end{pmatrix}. \quad (69)$$

808 The formulation (69) allows to explicitly characterize the irreversible dynamic
809 of SWE. Indeed, the last coordinate gives the precise expression of the in-
810 ternal entropy creation. For instance, when considering the Darcy-Weisbach
811 water-bed friction model $S = \frac{f_{DW} b |\alpha|}{8q}$, with f_{DW} the empirical friction coef-
812 ficient, the internal entropy creation is:

$$\partial_t s = \frac{S}{T} e_\alpha^2 = \frac{1}{T} \frac{f_{DW} b |\alpha|}{8q} \left(\frac{q\alpha}{\rho} \right)^2 \geq 0.$$

813 4.2. Irreversible port-Hamiltonian systems

814 IpH systems were defined [115] as an extension of pH systems for the
815 purpose of representing not only the energy balance but also the entropy
816 balance, essential in thermodynamics, as a structural property of a system.

817 The extension of this framework to infinite-dimensional systems defined on
818 1D spatial domains with first order differential operators was proposed in
819 [112] for a class of diffusion processes and generalized for a large class of
820 thermodynamic systems in [114]. The main feature of the IpH systems for-
821 mulation is that it precisely parametrizes the operators of (68) in terms of
822 the thermodynamic properties of a system such that, similar to pH systems,
823 the structure matrices of the system have a clear physical interpretation.

824 We shall define the following pseudo-brackets⁹ for any two functionals H_1
825 and H_2 of and for any matrix differential operator \mathcal{G} as:

$$\begin{aligned} \{H_1|\mathcal{G}|H_2\} &= \begin{bmatrix} \delta_{\mathbf{x}}H_1 \\ \delta_s H_1 \end{bmatrix} \cdot \begin{bmatrix} 0 & \mathcal{G} \\ -\mathcal{G}^* & 0 \end{bmatrix} \begin{bmatrix} \delta_{\mathbf{x}}H_2 \\ \delta_s H_2 \end{bmatrix}, \\ \{H_1|H_2\} &= \delta_s H_1^\top (\partial_\zeta \delta_s H_2), \end{aligned} \quad (70)$$

where \mathcal{G}^* denotes the formal adjoint operator of \mathcal{G} . An IpH system under-
going m irreversible processes on a 1D spatial domain is defined by a total
energy and total entropy functional, respectively H and S , a pair of matrices
 $P_0 = -P_0^\top \in \mathbb{R}^{n \times n}$, $P_1 = P_1^\top \in \mathbb{R}^{n \times n}$, $G_0 \in \mathbb{R}^{n \times m}$, $G_1 \in \mathbb{R}^{n \times m}$ with $m \leq n$
and the strictly positive real-valued functions $\gamma_{k,i}(\mathbf{x}, \zeta, \delta_{\mathbf{x}}H)$ $k = 0, 1$; $i \in$
 $\{1, \dots, m\}$, $\gamma_s(\mathbf{x}, \zeta, \delta_{\mathbf{x}}H) > 0$ and the PDE:

$$\begin{bmatrix} \partial_t \mathbf{x} \\ \partial_t s \end{bmatrix} = \begin{bmatrix} \mathcal{J} & \mathcal{G}_{\mathcal{R}} \\ \mathcal{G}_{\mathcal{R}}^* & \mathbf{r}_s \partial_\zeta + \partial_\zeta(\mathbf{r}_s \cdot) \end{bmatrix} \begin{bmatrix} \delta_{\mathbf{x}}H \\ \delta_s H \end{bmatrix},$$

826 where:

$$\mathcal{J} = P_0 + P_1 \partial_\zeta, \quad \mathcal{G}_{\mathcal{R}} = G_0 \mathbf{R}_0 + \partial_\zeta(G_1 \mathbf{R}_1 \cdot), \quad \mathcal{G}_{\mathcal{R}}^* = -\mathbf{R}^\top G_0^\top + \mathbf{R}_1^\top G_1^\top \partial_\zeta,$$

with vector-valued functions $\mathbf{R}_l(\mathbf{x}, \delta_{\mathbf{x}}H) \in \mathbb{R}^{m \times 1}$, $l = 0, 1$, defined by:

$$R_{0,i} = \gamma_{0,i}(\mathbf{x}, \zeta, \delta_{\mathbf{x}}H) \{S|G_0(:, i)|H\},$$

$$R_{1,i} = \gamma_{1,i}(\mathbf{x}, \zeta, \delta_{\mathbf{x}}H) \{S|G_1(:, i)\partial_\zeta|H\},$$

and:

$$r_s = \gamma_s(\mathbf{x}, \zeta, \delta_{\mathbf{x}}H) \{S|H\},$$

⁹the bracket is called a pseudo-bracket in the sense that the Jacobi-identity is not automatically satisfied, see e.g. [136, 126] for more details.

827 where the notation $G(:, i)$ indicates the i -th column of the matrix G . Here the
828 operator \mathcal{J} corresponds to the reversible coupling phenomena as it appears
829 in the example of the 1D SWE $P_0 = 0$ and: $P_1 = \begin{bmatrix} 0 & -1 \\ -1 & 0 \end{bmatrix}$. The operator
830 $\mathcal{G}_{\mathcal{R}}$ corresponds to the irreversible coupling phenomena. In the example of
831 the dissipative 1D SWE, $G_0 = 0$ and: $G_1 = \begin{bmatrix} 0 \\ 1 \end{bmatrix}$ which indicates that the
832 irreversible phenomenon associated with the friction of the fluid, couples
833 the momentum and the entropy balance equations. The functions $\gamma_{k,i}$ and
834 γ_s define the constitutive relations of the irreversible phenomena and the
835 functions $\{S|G_0(:, i)|H\}$, $\{S|G_1(:, i)\partial_\zeta|H\}$ and $\{S|H\}$ correspond to their
836 driving forces. In the example of the dissipative 1D SWE, $\{S|G_1(:, i)\partial_\zeta|H\} =$
837 $e_\alpha = \frac{q\alpha}{\rho}$ is indeed the driving force of the friction and $\gamma_{1,1} = \frac{S}{T}$ with $T = \delta_s H$
838 is indeed a strictly positive function containing the friction coefficient and
839 defining the constitutive relation of the friction model.

The previous definition is completed with port variables which enable to write the interaction of the system with its environment or other physical systems, in the manner as for dissipative pH systems as presented in Section 2.2. To this end, a Boundary Controlled IpH systems (BC-IPHS) is an infinite-dimensional IpH systems augmented with the boundary port variables:

$$v(t) = W_B \begin{bmatrix} e(L, t) \\ e(0, t) \end{bmatrix}, \quad y(t) = W_C \begin{bmatrix} e(L, t) \\ e(0, t) \end{bmatrix}, \quad (71)$$

840 as linear functions of the modified effort variable:

$$e(t, z) = \begin{bmatrix} \delta_{\mathbf{x}} H \\ \mathbf{R} \delta_s H \end{bmatrix}, \quad (72)$$

with $\mathbf{R} = [1 \quad \mathbf{R}_1 \quad \mathbf{r}_s]^\top$ and:

$$W_B = \begin{bmatrix} \frac{1}{\sqrt{2}} (\Xi_2 + \Xi_1 P_{ep}) M_p & \frac{1}{\sqrt{2}} (\Xi_2 - \Xi_1 P_{ep}) M_p \\ \frac{1}{\sqrt{2}} (\Xi_1 + \Xi_2 P_{ep}) M_p & \frac{1}{\sqrt{2}} (\Xi_1 - \Xi_2 P_{ep}) M_p \end{bmatrix},$$

$$W_C = \begin{bmatrix} \frac{1}{\sqrt{2}} (\Xi_1 + \Xi_2 P_{ep}) M_p & \frac{1}{\sqrt{2}} (\Xi_1 - \Xi_2 P_{ep}) M_p \end{bmatrix},$$

841 where $M_p = (M^\top M)^{-1} M^\top$, $P_{ep} = M^\top P_e M$ and $M \in \mathbb{R}^{(n+m+2) \times k}$ is span-

842 ning the columns of $P_e \in \mathbb{R}^{n+m+2}$ of rank k , defined by:

$$P_e = \begin{bmatrix} P_1 & 0 & G_1 & 0 \\ 0 & 0 & 0 & g_s \\ G_1^\top & 0 & 0 & 0 \\ 0 & g_s & 0 & 0 \end{bmatrix}, \quad (73)$$

and where Ξ_1 and Ξ_2 in $\mathbb{R}^{k \times k}$ satisfy $\Xi_2^\top \Xi_1 + \Xi_1^\top \Xi_2 = 0$ and $\Xi_2^\top \Xi_2 + \Xi_1^\top \Xi_1 = I$. Recalling the dissipative 1D SWE, its BC-IPHS formulation is obtained by completing the model with the boundary port variables:

$$v(t) = \begin{bmatrix} -e_q(L, t) + \frac{S}{T} e_\alpha(L, t) \\ e_q(0, t) - \frac{S}{T} e_\alpha(0, t) \end{bmatrix} = \begin{bmatrix} -\left(\frac{\alpha^2}{2\rho} + \frac{\rho g}{b} q\right)(L, t) + \frac{S}{T} \frac{q\alpha}{\rho}(L, t) \\ \left(\frac{\alpha^2}{2\rho} + \frac{\rho g}{b} q\right)(0, t) - \frac{S}{T} \frac{q\alpha}{\rho}(0, t) \end{bmatrix},$$

$$y(t) = \begin{bmatrix} e_\alpha(L, t) \\ e_\alpha(0, t) \end{bmatrix} = \begin{bmatrix} \frac{q\alpha}{\rho}(L, t) \\ \frac{q\alpha}{\rho}(0, t) \end{bmatrix}.$$

843 As for the reversible case, the boundary inputs and outputs correspond, re-
 844 spectively, to the pressure and the velocity evaluated at the boundary points
 845 0 and L . Note however that this time the pressure is the sum of the static and
 846 hydrodynamic pressures. If there is no dissipation in the system, $S = 0$, then
 847 the boundary inputs and outputs are exactly the same as for the reversible
 848 case.

849 BC-IPHS encode the first and second laws of Thermodynamics, *i.e.*, the
 850 conservation of the total energy and the irreversible production of entropy,
 851 as stated in the following lemmas [114, 113].

852 **Lemma (First law of Thermodynamics)**

The total energy balance is:

$$\dot{H} = y(t)^\top v(t),$$

853 which leads, when the input is set to zero, to $\dot{H} = 0$ in accordance with the
 854 first law of Thermodynamics.

855 **Lemma (Second law of Thermodynamics)**

The total entropy balance is given by:

$$\dot{S} = \int_{[0,L]} \sigma_t d\zeta - y_S^\top v_s,$$

856 where y_s and v_s are entropy conjugated input/output and σ_t is the total
857 internal entropy production. This leads, when the input is set to zero, to
858 $\dot{S} = \int_{[0,L]} \sigma_t d\zeta \geq 0$ in accordance with the second law of Thermodynamics.

859 *4.3. Multidimensional fluids and relation with metriplectic systems*

860 The infinite-dimensional IpH systems formulation has to date been de-
861 veloped for systems defined on 1D spatial domains. In [96] the pH systems
862 framework was applied to model 3D compressible fluids, both isentropic and
863 non-isentropic. For isentropic fluids, a dissipative pH system model that ac-
864 counts for the conversion of kinetic energy into heat due to viscous friction
865 was proposed, incorporating dissipative terms linked to the flow's vorticity
866 and compressibility. In scenarios involving fluid mixtures with multiple chem-
867 ical reactions under non-isentropic conditions, a quasi pH systems formula-
868 tion was employed to capture the dynamics and thermodynamic behavior of
869 the fluid. This approach involves defining specific operators and their formal
870 adjoints to characterize the various physical phenomena, including boundary
871 conditions related to the diffusion flux of matter. These results extended
872 previous pH systems formulations for non-isentropic 1D fluids [98, 4] to 2D
873 and 3D spatial domains, marking initial steps towards a general IpH systems
874 formulation for complex fluids and much in line with other geometrically
875 consistent thermodynamic formulations [27, 26, 25].

876 Recently, in [95] these developments were further generalized and formal-
877 ized to establish a comprehensive 1, 2, and 3D IpH systems formulation for
878 compressible fluids. This involves precise definition of operators that deter-
879 mine the IpH systems structure and boundary variables, ensuring compliance
880 with the first and the second law of Thermodynamics. The thermodynamic
881 formulation of fluids necessarily leads to the definition of metriplectic dynam-
882 ics [100] or similarly the GENERIC framework [62, 107]. This formulation is
883 a comprehensive approach in thermodynamics that aims at describing both
884 equilibrium and non-equilibrium systems. At its core it was proposed for
885 closed systems and consists of a reversible part that is governed by a Poisson
886 bracket, and an irreversible part governed by a dissipation bracket. These
887 two parts are connected via energy and co-energy variables that describe the

888 system. The reversible part captures the conservative dynamics typically
889 associated with Hamiltonian mechanics, while the irreversible part accounts
890 for dissipative phenomena, such as heat flow and viscous damping. By com-
891 bining these two aspects, GENERIC provides a unified description of the
892 dynamics of complex systems, encompassing both reversible and irreversible
893 processes, and can be applied to a wide range of physical situations, from
894 fluid dynamics to chemical reactions. There have been several studies in the
895 last decades extending GENERIC to open systems by establishing the link
896 of the formalism with other geometric approaches, such as the Matrix Model
897 [45, 74] and networked controlled systems defined by Dirac structures [75].
898 More recently, the link with dissipative pH systems have been established
899 in [102, 86] when considering the *Exergy* of a thermodynamic system as the
900 Hamiltonian function. Regarding numerical discretization schemes, recent
901 works have tackled the structure-preserving discretization in space and time
902 of metriplectic systems [127, 78, 143].

903 These results, which relate the different Hamiltonian-based formulations
904 are promising since they establish bridges between the approaches in terms
905 of fundamental thermodynamic principles, which are expected to help in the
906 developments and the extension of powerful proven numerical schemes such as
907 PFEM for quasi pH systems and IpH systems formulations of thermodynamic
908 systems.

909 **Conclusion and perspectives**

910 In conclusion, this paper has provided an extensive survey and analysis
911 of port-Hamiltonian formulations for the modeling and numerical simulation
912 of open-fluid systems.

913 The focal point of our discussion has been on the application of port-
914 Hamiltonian formulations to the shallow water equations and the incompress-
915 ible Navier-Stokes equations in 2D. Starting from the continuous formulation
916 with non-quadratic Hamiltonian, the application of a structure-preserving
917 method needed to be adapted with care, and was not straightforward con-
918 trarily to the linear quadratic features of structural mechanics: either a poly-
919 nomial nonlinearity or a differential linearity in the constitutive relation have
920 been successfully tackled. Through the presentation of numerical simulation
921 results for these specific cases, we have demonstrated the effectiveness of the
922 framework in capturing the essential dynamics of fluid systems.

923 Beyond these specific applications, our work has highlighted the broader
 924 implications of port-Hamiltonian formulations. Notably, it points towards
 925 promising research directions in the realm of thermodynamically-consistent
 926 modeling, structure-preserving numerical methods and also boundary control
 927 design for fluids. This, in turn, sets the stage for the simulation of complex
 928 fluid systems in interaction with their environment.

929 Addressing advanced constitutive laws, particularly for non-Newtonian
 930 fluids, stands as a significant challenge and an avenue for future investi-
 931 gation. Additionally, the intricate dynamics of fluid-structure interaction
 932 presents complexities, such as the interplay between Lagrangian and Eule-
 933 rian coordinates and the temporal evolution of the boundary between the
 934 fluid and the structure. Tackling these issues opens new frontiers for re-
 935 search, promising advances in our understanding and simulation capabilities
 936 for fluid systems.

937 **Acknowledgements**

938 The authors would like to warmly thank all the direct contributors to
 939 these works; first of all the Ph.D. students and post-doctoral researchers who
 940 have been working with lot of professionalism and enthusiasm on these topics,
 941 namely Andrea Brugnoli, Luis A. Mora, Anass Serhani, Saïd Aoues, Florian
 942 Monteghetti, Antoine Bendimerad-Hohl. They also want to thank their reg-
 943 ular collaborators for their contributions, insight and support, namely Paul
 944 Kotyczka, Laurent Lefèvre, Valérie Budinger, Daniel Alazard, Thomas Hélie,
 945 Michel Fournié. They are also very grateful to their colleagues that deeply
 946 contributed and put lot of energy to settle and move forward this field of re-
 947 search for their fruitful discussions and inspiration Bernhard Maschke, Arjan
 948 van der Schaft, Stefano Stramigioli, Hans Zwart, Volker Mehrmann among
 949 others.

950 **Appendix A. Some useful definitions**

Definition 3 (Formal adjoint). *Given a differential operator $\mathcal{A} : D(\mathcal{A}) \subset \mathcal{X} \rightarrow \mathcal{Y}$, where \mathcal{X} and \mathcal{Y} are two Hilbert spaces (of functions), the formal adjoint \mathcal{A}^* of \mathcal{A} is defined as:*

$$\int_{\Omega} \mathcal{A}\varphi \cdot \psi \, d\Omega =: \int_{\Omega} \varphi \cdot \mathcal{A}^*\psi \, d\Omega, \quad \forall \varphi, \psi \in \mathcal{C}_c^\infty(\Omega),$$

951 where $\mathcal{C}_c^\infty(\Omega)$ is the space of compactly-supported infinitely differentiable func-
 952 tions.

Definition 4 (Formal skew-symmetry). A differential operator $\mathcal{J} : D(\mathcal{J}) \subset \mathcal{X} \rightarrow \mathcal{X}$ is formally skew-symmetric if:

$$\int_{\Omega} \mathcal{J}\varphi \cdot \psi \, d\Omega =: - \int_{\Omega} \varphi \cdot \mathcal{J}\psi \, d\Omega, \quad \forall \varphi, \psi \in \mathcal{C}_c^\infty(\Omega).$$

Definition 5 (Dirac structure). Given a Hilbert space \mathcal{E} , called the effort space, and its topological dual¹⁰ $\mathcal{F} := \mathcal{E}'$, called the flow space, we define the Bond space $\mathcal{B} := \mathcal{F} \times \mathcal{E}$ endowed with the bilinear symmetric product:

$$\left\langle \left\langle \begin{pmatrix} f^1 \\ e^1 \end{pmatrix}, \begin{pmatrix} f^2 \\ e^2 \end{pmatrix} \right\rangle \right\rangle_{\mathcal{B}} := \langle f^1, e^2 \rangle_{\mathcal{F}, \mathcal{E}} + \langle f^2, e^1 \rangle_{\mathcal{F}, \mathcal{E}},$$

where $\langle \cdot, \cdot \rangle_{\mathcal{F}, \mathcal{E}}$ represents the duality bracket. A (Stokes-)Dirac structure is a subspace $\mathcal{D} \subset \mathcal{B}$ which is maximal isotropic in \mathcal{B} , i.e. it satisfies:

$$\mathcal{D}^\top = \mathcal{D},$$

953 where \mathcal{D}^\top is the orthogonal companion of \mathcal{D} in \mathcal{B} with respect to the Bond
 954 product $\langle \langle \cdot, \cdot \rangle \rangle_{\mathcal{B}}$.

Remark 17. An important result in finite dimension is the kernel representation of a Dirac structure [125, § 5.1] which states that a Dirac structure always admits two matrices E and F of appropriate dimension such that:

$$\mathcal{D} = \left\{ \begin{pmatrix} f \\ e \end{pmatrix} \in \mathcal{B} \mid Ff + Ee = 0 \right\}.$$

955 After discretization, see Section 3, we are essentially concerned with the case
 956 $F^\top = F > 0$ and $E^\top = -E$ in the sequel. In that case, E is often denoted J
 957 and is called the structure matrix. We abuse the language and will talk about
 958 structure operator in the infinite-dimensional case.

959 **Remark 18.** In infinite dimensions, a Dirac structure is rather called a
 960 Stokes-Dirac structure, in order to emphasize that its structure operator is
 961 formally skew-symmetric thanks to the Stokes's divergence theorem.

¹⁰In finite dimension, the definition is often written in the other way: $\mathcal{E} := \mathcal{F}'$.

962 **Remark 19.** *Rigorously, the Bond product makes use of the duality bracket*
963 *between \mathcal{E} and \mathcal{F} . In this work, we will always assume a strong regularity*
964 *(i.e. at least C^1 in space and time) for the solutions to a pH system. In that*
965 *case, this duality bracket reduces to a more convenient L^2 -inner product over*
966 *the spatial domain Ω . Moreover, the boundary traces of such solutions are*
967 *then sufficiently regular to allow also the identification of the duality bracket*
968 *at the boundary of Ω by the L^2 -inner product at the boundary.*

969 Appendix B. Proof of some theorems

970 Appendix B.1. Proof of Theorem 2

Along the trajectories of system (31), one has:

$$\begin{aligned}
\dot{\mathcal{H}} &= \int_{\Omega} \partial_t \mathbf{u} \cdot \delta_{\mathbf{u}} \mathcal{H} \, d\Omega, \\
&= \int_{\Omega} \partial_t \mathbf{u} \cdot (\rho_0 \mathbf{u}) \, d\Omega, \\
&= \int_{\Omega} \rho_0 \partial_t \mathbf{u} \cdot \mathbf{u} \, d\Omega, \\
&= \int_{\Omega} (G(\boldsymbol{\omega}) \mathbf{u} \cdot \mathbf{u} - \mathbf{curl}(\mathbf{e}_c) \cdot \mathbf{u} + \mathbf{grad}(\mathbf{e}_d) \cdot \mathbf{u}) \, d\Omega, \\
&= \underbrace{\int_{\Omega} G(\boldsymbol{\omega}) \mathbf{u} \cdot \mathbf{u} \, d\Omega}_{=0} - \int_{\Omega} \mathbf{e}_c \cdot \mathbf{curl}(\mathbf{u}) \, d\Omega - \int_{\partial\Omega} \mathbf{e}_c \cdot (\mathbf{u} \wedge \mathbf{n}) \, d\gamma \\
&\quad - \int_{\Omega} \mathbf{e}_d \underbrace{\operatorname{div}(\mathbf{u})}_{=0} \, d\Omega + \int_{\partial\Omega} \mathbf{e}_d \mathbf{u} \cdot \mathbf{n} \, d\gamma, \\
&= - \int_{\Omega} \mathbf{e}_c \cdot \mathbf{f}_c \, d\Omega - \int_{\partial\Omega} \mathbf{e}_c \cdot (\mathbf{u} \wedge \mathbf{n}) \, d\gamma + \int_{\partial\Omega} \mathbf{e}_d \mathbf{u} \cdot \mathbf{n} \, d\gamma, \\
&= - \int_{\Omega} \mathbf{e}_c \cdot \mathbf{f}_c \, d\Omega + \int_{\partial\Omega} (\mathbf{e}_d \mathbf{u} \cdot \mathbf{n} - \mathbf{e}_c \cdot (\mathbf{u} \wedge \mathbf{n})) \, d\gamma, \\
&= - \int_{\Omega} \mu_c \|\boldsymbol{\omega}\|^2 \, d\Omega + \int_{\partial\Omega} \left(\left(P + \frac{1}{2} \rho_0 \|\mathbf{u}\|^2 \right) \mathbf{u} \cdot \mathbf{n} - \mu_c \boldsymbol{\omega} \cdot (\mathbf{u} \wedge \mathbf{n}) \right) \, d\gamma.
\end{aligned}$$

971 *Appendix B.2. Proof of Theorem 6*

Along the trajectories of system (36), one has:

$$\begin{aligned}
\dot{\mathcal{H}} &= \int_{\Omega} \rho_0 \partial_t \omega \delta_{\omega}^{\rho_0} \mathcal{H} \, d\Omega, \\
&= \int_{\Omega} \rho_0 \partial_t \omega \psi \, d\Omega, \\
&= \int_{\Omega} (J_{\omega} \psi - \text{curl}_{2D} \mathbf{grad}^{\perp}(e_c)) \psi \, d\Omega, \\
&= \int_{\Omega} \text{curl}_{2D} (G(\omega) \mathbf{grad}^{\perp}(\psi)) \psi \, d\Omega - \int_{\Omega} \text{curl}_{2D} \mathbf{grad}^{\perp}(e_c) \psi \, d\Omega, \\
&= \int_{\Omega} \underbrace{G(\omega) \mathbf{grad}^{\perp}(\psi) \cdot \mathbf{grad}^{\perp}(\psi)}_{=0} \, d\Omega + \int_{\partial\Omega} \underbrace{\Theta G(\omega)}_{=\omega I_2} \mathbf{grad}^{\perp}(\psi) \cdot \mathbf{n} \, d\gamma \\
&\quad - \int_{\Omega} \mathbf{grad}^{\perp}(e_c) \cdot \mathbf{grad}^{\perp}(\psi) \, d\Omega - \int_{\partial\Omega} \Theta \mathbf{grad}^{\perp}(e_c) \cdot \mathbf{n} \, d\gamma, \\
&= \int_{\partial\Omega} \omega \psi \mathbf{grad}^{\perp}(\psi) \cdot \mathbf{n} \, d\gamma - \int_{\Omega} \underbrace{e_c}_{=\mu_c \omega} \underbrace{\text{curl}_{2D} \mathbf{grad}^{\perp}(\psi)}_{=\omega} \, d\Omega \\
&\quad + \int_{\partial\Omega} \underbrace{\Theta \mathbf{grad}^{\perp}(\psi)}_{=-\mathbf{grad}(\psi)} \cdot \mathbf{n} e_c \, d\gamma - \int_{\partial\Omega} \underbrace{\mathcal{R} \mathbf{grad}^{\perp}(e_c)}_{=-\mathbf{grad}(\mu_c \omega)} \cdot \mathbf{n} \, d\gamma,
\end{aligned}$$

972 hence the result.

973 *Appendix B.3. Proof of Theorem 8*

First, note that, using the symmetry of the matrices $Q_{\alpha}[\underline{h}(t)]$ and Q_h appearing in the definition of the discrete Hamiltonian \mathcal{H}^d given in (43):

$$\begin{aligned}
\frac{d}{dt} \mathcal{H}^d(\underline{h}(t), \underline{\alpha}(t)) &= \underline{\alpha}(t)^{\top} Q_{\alpha}[\underline{h}(t)] \frac{d}{dt} \underline{\alpha}(t) + \underline{h}(t)^{\top} Q_h \frac{d}{dt} \underline{h}(t) \\
&\quad + \frac{1}{2} \underline{\alpha}(t)^{\top} \frac{d}{dt} Q_{\alpha}[\underline{h}(t)] \underline{\alpha}(t). \quad (\text{B.1})
\end{aligned}$$

On the other hand, multiplying (41) by $(\underline{e}_h(t)^{\top} \quad \underline{e}_{\alpha}(t)^{\top} \quad \underline{e}_{\partial}(t)^{\top})^{\top}$ by the left leads to:

$$\begin{aligned}
&\underline{e}_h(t)^{\top} M_h \frac{d}{dt} \underline{h}(t) + \underline{e}_{\alpha}(t)^{\top} M_{\alpha} \frac{d}{dt} \underline{\alpha}(t) - \underline{e}_{\partial}(t)^{\top} M_{\partial} \underline{f}_{\partial}(t) \\
&= \underline{e}_h(t)^{\top} D \underline{e}_{\alpha}(t) + \underline{e}_h(t)^{\top} B \underline{e}_{\partial}(t) - \underline{e}_{\alpha}(t)^{\top} D^{\top} \underline{e}_h(t) - \underline{e}_{\partial}(t)^{\top} B^{\top} \underline{e}_h(t),
\end{aligned}$$

which simplifies into:

$$\underline{e}_h(t)^\top M_h \frac{d}{dt} \underline{h}(t) + \underline{e}_\alpha(t)^\top M_\alpha \frac{d}{dt} \underline{\alpha}(t) = \underline{e}_\partial(t)^\top M_\partial \underline{f}_\partial(t).$$

Now, since the mass matrices are symmetric, one can make use of (42) to get:

$$(Q_h \underline{h}(t) + N[\underline{\alpha}(t)] \underline{\alpha}(t))^\top \frac{d}{dt} \underline{h}(t) + (Q_\alpha[\underline{h}(t)] \underline{\alpha}(t))^\top \frac{d}{dt} \underline{\alpha}(t) = \underline{e}_\partial(t)^\top M_\partial \underline{f}_\partial(t),$$

or, after rearranging the terms and taking advantage of the symmetry of the Q matrices:

$$\begin{aligned} \underline{\alpha}(t)^\top N[\underline{\alpha}(t)]^\top \frac{d}{dt} \underline{h}(t) + \underline{h}(t)^\top Q_h \frac{d}{dt} \underline{h}(t) \\ + \underline{\alpha}(t)^\top Q_\alpha[\underline{h}(t)] \frac{d}{dt} \underline{\alpha}(t) = \underline{e}_\partial(t)^\top M_\partial \underline{f}_\partial(t). \end{aligned}$$

Combining the latter with (B.1) gives:

$$\begin{aligned} \frac{d}{dt} \mathcal{H}^d(\underline{h}(t), \underline{\alpha}(t)) = \underline{e}_\partial(t)^\top M_\partial \underline{f}_\partial(t) \\ + \frac{1}{2} \underline{\alpha}(t)^\top \frac{d}{dt} Q_\alpha[\underline{h}(t)] \underline{\alpha}(t) - \underline{\alpha}(t)^\top N[\underline{\alpha}(t)]^\top \frac{d}{dt} \underline{h}(t). \end{aligned}$$

Once again, the fact that the Hamiltonian is polynomial is crucial (compare the following with the equality in Remark 12), since it leads straightforwardly to:

$$\frac{1}{2} \underline{\alpha}(t)^\top \frac{d}{dt} Q_\alpha[\underline{h}(t)] \underline{\alpha}(t) = \underline{\alpha}(t)^\top N[\underline{\alpha}(t)]^\top \frac{d}{dt} \underline{h}(t),$$

974 hence, to the result.

975 *Appendix B.4. Proof of Theorem 10*

Let us multiply (60) by $(\underline{\psi}^\top \ \underline{e}_c^\top \ \underline{u}_n^\top \ \underline{u}_\tau^\top \ \underline{\dot{u}}_\tau^\top \ \underline{y}_c^\top)^\top$ by the left. Then:

$$\underline{\psi}^\top M_\psi \dot{\underline{\psi}} + \underline{e}_c^\top M_c \underline{e}_c - \underline{u}_n^\top M_\partial \underline{y}_n - \underline{u}_\tau^\top M_\partial \underline{y}_\tau - \underline{\dot{u}}_\tau^\top M_\partial \underline{y}_{dt} - \underline{y}_c^\top M_\partial \underline{u}_c = 0.$$

After rearrangement, it reads:

$$\underline{\psi}^\top M_\psi \dot{\underline{\psi}} - \underline{\dot{u}}_\tau^\top M_\partial \underline{y}_{dt} = -\underline{e}_c^\top M_c \underline{e}_c + \underline{u}_n^\top M_\partial \underline{y}_n + \underline{u}_\tau^\top M_\partial \underline{y}_\tau + \underline{y}_c^\top M_\partial \underline{u}_c.$$

Now, with the discrete Hamiltonian \mathcal{H}^d , given in (61), let us show that $\frac{d}{dt}\mathcal{H}^d(\underline{\omega}) = \underline{\psi}^\top M_\psi \dot{\underline{\psi}} - \underline{\dot{u}}_\tau^\top M_{\partial} \underline{y}_{dt}$. As in the continuous case, the difficulty relies on the fact that \mathcal{H}^d is defined as a function of $\underline{\omega}$, hence:

$$\frac{d}{dt}\mathcal{H}^d(\underline{\omega}) = \nabla_{\underline{\omega}}\mathcal{H}^d(\underline{\omega}) \cdot \dot{\underline{\omega}},$$

976 and one requires to compute the gradient of the Hamiltonian with respect
 977 to the energy variable $\underline{\omega}$. Let us compute it in the distributional sense,
 978 following [106] at the continuous level, as in Proposition 4.

Let $\underline{w} \in \mathbb{R}^{N_c}$ be such that $w^d(\boldsymbol{\zeta}, t) = \sum_{k=1}^{N_c} w^k \Phi^k(\boldsymbol{\zeta})$ is compactly supported and in the range of curl_{2D} , *i.e.*, there exists $\boldsymbol{\eta}^d \in (L^2(\Omega))^2$ compactly supported and satisfying $\text{curl}_{2D}\boldsymbol{\eta}^d = w^d$. Then, for all $\varepsilon > 0$:

$$\begin{aligned} \frac{\mathcal{H}^d(\underline{\omega} + \varepsilon\underline{w}) - \mathcal{H}^d(\underline{\omega})}{\varepsilon} &= \frac{1}{2\varepsilon} \int_{\Omega} \rho_0 \|\mathbf{u}^d + \varepsilon\boldsymbol{\eta}^d\|^2 d\Omega - \frac{1}{2\varepsilon} \int_{\Omega} \rho_0 \|\mathbf{u}^d\|^2 d\Omega, \\ &= \int_{\Omega} \rho_0 \mathbf{u}^d \cdot \boldsymbol{\eta}^d d\Omega + O(\varepsilon). \end{aligned}$$

Using $\mathbf{u}^d = \mathbf{grad}^\perp(\psi^d)$ and applying the integration by part (33) leads to:

$$\nabla_{\underline{\omega}}\mathcal{H}^d(\underline{\omega}) \cdot \underline{w} = \int_{\Omega} \rho_0 \psi^d w^d d\Omega,$$

from which we recover that $\rho_0\underline{\psi}$ is indeed the co-energy variable at the discrete level, as expected. Now:

$$\begin{aligned} \nabla_{\underline{\omega}}\mathcal{H}^d(\underline{\omega}) \cdot \dot{\underline{\omega}} &= \int_{\Omega} \rho_0 \psi^d \partial_t \omega^d d\Omega, \\ &= - \int_{\Omega} \rho_0 \psi^d \partial_t (\Delta \psi^d) d\Omega, \\ &= - \int_{\Omega} \rho_0 \psi^d \Delta (\partial_t \psi^d) d\Omega, \\ &= - \int_{\Omega} \rho_0 \psi^d \text{div} \mathbf{grad} (\partial_t \psi^d) d\Omega, \\ &= \int_{\Omega} \rho_0 \mathbf{grad}(\psi^d) \cdot \mathbf{grad}(\partial_t \psi^d) d\Omega \\ &\quad - \int_{\partial\Omega} \rho_0 \psi^d \mathbf{grad}(\partial_t \psi^d) \cdot \mathbf{n} d\gamma, \\ &= \int_{\Omega} \rho_0 \mathbf{grad}(\psi^d) \cdot \mathbf{grad}(\partial_t \psi^d) d\Omega - \int_{\partial\Omega} \rho_0 \psi^d \partial_t u_\tau d\gamma, \\ &= \underline{\psi}^\top M_\psi \dot{\underline{\psi}} - \underline{\psi}^\top B_{dt}^\top \underline{\dot{u}}_\tau, \end{aligned}$$

979 hence the result, since $B_{dt} \underline{\psi} = M_{\partial} \underline{y}_{dt}$, and M_{∂} is symmetric.

980 References

- 981 [1] Abhyankar, S., Brown, J., Constantinescu, E.M., Ghosh, D., Smith,
982 B.F., Zhang, H., 2018. PETSc/TS: A Modern Scalable ODE/DAE
983 Solver Library. Technical Report. arXiv:1806.01437.
- 984 [2] Alonso, A.A., Ydstie, B.E., Banga, J.R., 2002. From irreversible ther-
985 modynamics to a robust control theory for distributed process systems.
986 Journal of Process Control 12, 507–517. doi:10.1016/S0959-1524(01)
987 00017-8.
- 988 [3] Altmann, R., Mehrmann, V., Unger, B., 2021. Port-Hamiltonian for-
989 mulations of poroelastic network models. Mathematical and Computer
990 Modelling of Dynamical Systems 27, 429–452. doi:10.1080/13873954.
991 2021.1975137.
- 992 [4] Altmann, R., Schulze, P., 2017. A port-Hamiltonian formulation of the
993 Navier–Stokes equations for reactive flows. Systems & Control Letters
994 100, 51–55. doi:10.1016/j.sysconle.2016.12.005.
- 995 [5] Aoues, S., Cardoso-Ribeiro, F.L., Matignon, D., Alazard, D., 2017.
996 Modeling and control of a rotating flexible spacecraft: A port-
997 Hamiltonian approach. IEEE Transactions on Control Systems Tech-
998 nology 27, 355–362. doi:10.1109/TCST.2017.2771244.
- 999 [6] Arnold, D., Falk, R., Winther, R., 2010. Finite element exter-
1000 ior calculus: from Hodge theory to numerical stability. Bulletin
1001 of the American Mathematical Society 47, 281–354. doi:10.1090/
1002 s0273-0979-10-01278-4.
- 1003 [7] Arnold, D.N., Falk, R.S., Winther, R., 2006. Finite element exterior
1004 calculus, homological techniques, and applications. Acta Numerica 15,
1005 1–155. doi:10.1017/S0962492906210018.
- 1006 [8] Beattie, C., Mehrmann, V., Xu, H., Zwart, H., 2018. Linear port-
1007 Hamiltonian descriptor systems. Mathematics of Control, Signals, and
1008 Systems 30, 1–27. doi:10.1007/s00498-018-0223-3.

- 1009 [9] Bendimerad-Hohl, A., Haine, G., Lefèvre, L., Matignon, D., 2023a.
1010 Implicit port-Hamiltonian systems: structure-preserving discretization
1011 for the nonlocal vibrations in a viscoelastic nanorod, and for a seepage
1012 model. *IFAC-PapersOnLine* 56, 6789–6795. doi:10.1016/j.ifacol.
1013 2023.10.387. 22nd IFAC World Congress.
- 1014 [10] Bendimerad-Hohl, A., Haine, G., Matignon, D., 2023b. Structure-
1015 preserving discretization of the Cahn-Hilliard equations recast as
1016 a port-Hamiltonian system, in: *Geometric Science of Information*.
1017 Springer, Cham, pp. 192–201. doi:10.1007/978-3-031-38299-4_21.
- 1018 [11] Bendimerad-Hohl, A., Haine, G., Matignon, D., Maschke, B., 2022.
1019 Structure-preserving discretization of a coupled Allen-Cahn and heat
1020 equation system. *IFAC-PapersOnLine* 55, 99–104. doi:10.1016/j.
1021 ifacol.2022.08.037.
- 1022 [12] Benner, P., Goyal, P., Van Dooren, P., 2020. Identification of port-
1023 Hamiltonian systems from frequency response data. *Systems & Control*
1024 *Letters* 143, 104741. doi:https://doi.org/10.1016/j.sysconle.
1025 2020.104741.
- 1026 [13] Bird, R.B., 2002. Transport phenomena. *Applied Mechanics Reviews*
1027 55, R1–R4. doi:10.1115/1.1424298.
- 1028 [14] Bochev, P.B., Hyman, J.M., 2006. Principles of mimetic discretiza-
1029 tions of differential operators, in: Arnold, D., Bochev, P., Lehoucq,
1030 R., Nicolaides, R., Shashkov, M. (Eds.), *Compatible Spatial Dis-*
1031 *cretizations*. Springer Verlag, Berlin. volume 142 of *IMA*, pp. 89–119.
1032 doi:10.1007/0-387-38034-5_5.
- 1033 [15] Boffi, D., Brezzi, F., Fortin, M., 2015. *Mixed Finite Element Meth-*
1034 *ods and Applications*. Springer, Berlin, Heidelberg. doi:10.1007/
1035 978-3-642-36519-5.
- 1036 [16] Boyer, F., Fabrie, P., 2013. Mathematical tools for the study of the
1037 incompressible Navier-Stokes equations and related models. volume 183
1038 of *Applied Mathematical Sciences*. Springer, New York. doi:10.1007/
1039 978-1-4614-5975-0.
- 1040 [17] Brayton, R., Moser, J., 1964. A theory of nonlinear networks. I. *Quar-*
1041 *terly of Applied Mathematics* 22, 1–33.

- 1042 [18] Brugnoli, A., Alazard, D., Pommier-Budinger, V., Matignon, D.,
1043 2019a. Port-Hamiltonian formulation and symplectic discretization of
1044 plate models Part I: Mindlin model for thick plates. *Applied Mathe-*
1045 *matical Modelling* 75, 940–960. doi:10.1016/j.apm.2019.04.035.
- 1046 [19] Brugnoli, A., Alazard, D., Pommier-Budinger, V., Matignon, D.,
1047 2019b. Port-Hamiltonian formulation and symplectic discretization of
1048 plate models Part II: Kirchhoff model for thin plates. *Applied Mathe-*
1049 *matical Modelling* 75, 961–981. doi:10.1016/j.apm.2019.04.036.
- 1050 [20] Brugnoli, A., Cardoso-Ribeiro, F.L., Haine, G., Kotyczka, P., 2020.
1051 Partitioned finite element method for structured discretization with
1052 mixed boundary conditions. *IFAC-PapersOnLine* 53, 7557–7562.
1053 doi:10.1016/j.ifacol.2020.12.1351. 21st IFAC World Congress.
- 1054 [21] Brugnoli, A., Haine, G., Matignon, D., 2022a. Explicit structure-
1055 preserving discretization of port-Hamiltonian systems with mixed
1056 boundary control. *IFAC-PapersOnLine* 55, 418–423. doi:10.1016/j.
1057 *ifacol.2022.11.089*. 25th International Symposium on Mathemati-
1058 *cal Theory of Networks and Systems MTNS 2022*.
- 1059 [22] Brugnoli, A., Haine, G., Matignon, D., 2023. Stokes-Dirac structures
1060 for distributed parameter port-Hamiltonian systems: An analytical
1061 viewpoint. *Communications in Analysis and Mechanics* 15, 362–387.
1062 doi:10.3934/cam.2023018.
- 1063 [23] Brugnoli, A., Haine, G., Serhani, A., Vasseur, X., 2021. Numerical
1064 approximation of port-Hamiltonian systems for hyperbolic or parabolic
1065 PDEs with boundary control. *Journal of Applied Mathematics and*
1066 *Physics* 9, 1278–1321. doi:10.4236/jamp.2021.96088. supplementary
1067 material, <https://doi.org/10.5281/zenodo.3938600>.
- 1068 [24] Brugnoli, A., Rashad, R., Stramigioli, S., 2022b. Dual field structure-
1069 preserving discretization of port-Hamiltonian systems using finite ele-
1070 ment exterior calculus. *Journal of Computational Physics* 471, 111601.
1071 doi:10.1016/j.jcp.2022.111601.
- 1072 [25] Califano, F., Rashad, R., Schuller, F.P., Stramigioli, S., 2021. Ge-
1073 ometric and energy-aware decomposition of the Navier–Stokes equa-
1074 tions: A port-Hamiltonian approach. *Physics of Fluids* 33, 047114.
1075 doi:10.1063/5.0048359.

- 1076 [26] Califano, F., Rashad, R., Schuller, F.P., Stramigioli, S., 2022a. Energetic decomposition of distributed systems with moving material domains: the port-Hamiltonian model of fluid-structure interaction. *Journal of Geometry and Physics* 175, 104477. doi:10.1016/j.geomphys.2022.104477.
- 1077
1078
1079
1080
- 1081 [27] Califano, F., Rashad, R., Stramigioli, S., 2022b. A differential geometric description of thermodynamics in continuum mechanics with application to Fourier–Navier–Stokes fluids. *Physics of Fluids* 34, 107113. doi:10.1063/5.0119517.
- 1082
1083
1084
- 1085 [28] Cardoso-Ribeiro, F.L., Brugnoli, A., Matignon, D., Lefèvre, L., 2019. Port-Hamiltonian modeling, discretization and feedback control of a circular water tank, in: 2019 IEEE 58th Conference on Decision and Control (CDC), pp. 6881–6886. doi:10.1109/CDC40024.2019.9030007.
- 1086
1087
1088
1089
- 1090 [29] Cardoso-Ribeiro, F.L., Haine, G., Lefèvre, L., Matignon, D., 2023. Rotational Shallow Water Equations with viscous damping and boundary control: structure-preserving spatial discretization. PREPRINT Available at Research Square doi:10.21203/rs.3.rs-3006274/v2.
- 1091
1092
1093
- 1094 [30] Cardoso-Ribeiro, F.L., Matignon, D., Lefèvre, L., 2021a. A Partitioned Finite-Element Method for power-preserving discretization of open systems of conservation laws. *IMA J. Mathematical Control and Information* 38, 493–533. doi:10.1093/imamci/dnaa038.
- 1095
1096
1097
- 1098 [31] Cardoso-Ribeiro, F.L., Matignon, D., Lefèvre, L., 2021b. Dissipative Shallow Water Equations: a port-Hamiltonian formulation. *IFAC-PapersOnLine* 54, 167–172. doi:https://doi.org/10.1016/j.ifacol.2021.11.073. 7th IFAC Workshop on Lagrangian and Hamiltonian Methods for Nonlinear Control LHMNC 2021.
- 1099
1100
1101
1102
- 1103 [32] Cardoso-Ribeiro, F.L., Matignon, D., Pommier-Budinger, V., 2017. A port-Hamiltonian model of liquid sloshing in moving containers and application to a fluid-structure system. *Journal of Fluids and Structures* 69, 402–427. doi:10.1016/j.jfluidstructs.2016.12.007.
- 1104
1105
1106
- 1107 [33] Cardoso-Ribeiro, F.L., Matignon, D., Pommier-Budinger, V., 2020. Port-Hamiltonian model of two-dimensional shallow water equations
- 1108

- 1109 in moving containers. IMA Journal of Mathematical Control and In-
1110 formation 37, 1348–1366. doi:10.1093/imamci/dnaa016.
- 1111 [34] Cervera, J., van der Schaft, A., Baños, A., 2007. Interconnection of
1112 port-Hamiltonian systems and composition of Dirac structures. Auto-
1113 matica 43, 212–225. doi:10.1016/j.automatica.2006.08.014.
- 1114 [35] Chorin, A.J., Marsden, J.E., 1992. A Mathematical Introduction to
1115 Fluid Mechanics. volume 4 of *Texts in Applied Mathematics*. Springer,
1116 New York. doi:10.1007/978-1-4612-0883-9.
- 1117 [36] Cisneros, N., Rojas, A.J., Ramirez, H., 2020. Port-Hamiltonian Model-
1118 ing and Control of a Micro-Channel Experimental Plant. IEEE Access
1119 8, 176935–176946. doi:10.1109/ACCESS.2020.3026653.
- 1120 [37] Cotter, C.J., 2023. Compatible finite element methods for geophys-
1121 ical fluid dynamics. Acta Numerica 32, 291–393. doi:10.1017/
1122 S0962492923000028.
- 1123 [38] Courant, T.J., 1990. Dirac manifolds. Transactions of the
1124 American Mathematical Society 319, 631–661. doi:10.1090/
1125 S0002-9947-1990-0998124-1.
- 1126 [39] De Groot, S.R., Mazur, P., 2013. Non-equilibrium thermodynamics.
1127 Courier Corporation.
- 1128 [40] Diab, M., Tischendorf, C., 2021. Splitting methods for linear circuit
1129 DAEs of index 1 in port-Hamiltonian form, in: van Beurden, M.,
1130 Budko, N., Schilders, W. (Eds.), *Scientific Computing in Electrical
1131 Engineering*, Springer International Publishing, Cham. pp. 211–219.
1132 doi:10.1007/978-3-030-84238-3_21.
- 1133 [41] Domschke, P., Hiller, B., Lang, J., Mehrmann, V., Morandin, R., Tis-
1134 chendorf, C., 2021. Gas Network Modeling: An Overview. Technical
1135 Report. Technische Universität Darmstadt. URL: [https://opus4.
1136 kobv.de/opus4-trr154/frontdoor/index/index/docId/411](https://opus4.kobv.de/opus4-trr154/frontdoor/index/index/docId/411).
- 1137 [42] Dubljevic, S., 2022. Quo Vadis Advanced Chemical Process Control.
1138 The Canadian Journal of Chemical Engineering 100, 2135. doi:10.
1139 1002/cjce.24505.

- 1140 [43] Duindam, V., Macchelli, A., Stramigioli, S., Bruyninckx, H., 2009.
 1141 Modeling and Control of Complex Physical Systems: The Port-
 1142 Hamiltonian Approach. Springer, Berlin, Heidelberg. doi:10.1007/
 1143 978-3-642-03196-0.
- 1144 [44] Eberard, D., Maschke, B.M., van der Schaft, A.J., 2007. An extension
 1145 of Hamiltonian systems to the thermodynamic phase space: Towards a
 1146 geometry of nonreversible processes. Reports on Mathematical Physics
 1147 60, 175–198. doi:10.1016/S0034-4877(07)00024-9.
- 1148 [45] Edwards, B.J., Öttinger, H.C., Jongschaap, R.J.J., 1997. On the
 1149 relationships between thermodynamic formalisms for complex fluids.
 1150 Journal of Non-Equilibrium Thermodynamics 22, 356–373. doi:doi:
 1151 10.1515/jnet.1997.22.4.356.
- 1152 [46] Egger, H., 2019. Structure preserving approximation of dissipative
 1153 evolution problems. Numerische Mathematik 143, 85–106. doi:10.
 1154 1007/s00211-019-01050-w.
- 1155 [47] Emmrich, E., Mehrmann, V., 2013. Operator differential-algebraic
 1156 equations arising in fluid dynamics. Computational Methods in Ap-
 1157 plied Mathematics 13, 443–470. doi:10.1515/cmam-2013-0022.
- 1158 [48] Erbay, M., Jacob, B., Morris, K., 2024a. On the Weierstraß form of in-
 1159 finite dimensional differential algebraic equations. arXiv:2402.17560.
- 1160 [49] Erbay, M., Jacob, B., Morris, K., Reis, T., Tischendorf, C., 2024b.
 1161 Index concepts for linear differential-algebraic equations in finite and
 1162 infinite dimensions. arXiv:2401.01771.
- 1163 [50] Farle, O., Baltes, R.B., Dyczij-Edlinger, R., 2014a. A port-Hamiltonian
 1164 finite-element formulation for the transmission line, in: Proceedings of
 1165 21st International Symposium on Mathematical Theory of Networks
 1166 and Systems, pp. 724–728.
- 1167 [51] Farle, O., Baltes, R.B., Dyczij-Edlinger, R., 2014b. Strukturerehal-
 1168 tende Diskretisierung verteilt-parametrischer Port-Hamiltonscher Sys-
 1169 teme mittels finiter Elemente. at-Automatisierungstechnik 62, 500–511.
 1170 doi:10.1515/auto-2014-1093.

- 1171 [52] Farle, O., Klis, D., Jochum, M., Floch, O., Dyczij-Edlinger, R., 2013. A
1172 port-Hamiltonian finite-element formulation for the Maxwell equations,
1173 in: 2013 International Conference on Electromagnetics in Advanced
1174 Applications (ICEAA), IEEE. pp. 324–327. doi:10.1109/ICEAA.2013.
1175 6632246.
- 1176 [53] Ferraro, G., Fournié, M., Haine, G., . Simulation and control of inter-
1177 actions in multi-physics, a Python package for port-Hamiltonian sys-
1178 tems. Accepted for presentation at IFAC LHMNC 2024, Besançon,
1179 France.
- 1180 [54] Gawlik, E.S., Gay-Balmaz, F., 2021. A Variational Finite Element
1181 Discretization of Compressible Flow. *Foundations of Computational*
1182 *Mathematics* 21, 961–1001. doi:10.1007/s10208-020-09473-w.
- 1183 [55] Gay-Balmaz, F., Yoshimura, H., 2018. A Variational Formulation
1184 of Nonequilibrium Thermodynamics for Discrete Open Systems with
1185 Mass and Heat Transfer. *Entropy* 20, 163. doi:10.3390/e20030163.
- 1186 [56] Gerbeau, J.F., Perthame, B., 2001. Derivation of viscous Saint-Venant
1187 system for laminar shallow water; Numerical validation. *Discrete and*
1188 *Continuous Dynamical Systems - B* 1, 89–102. doi:10.3934/dcdsb.
1189 2001.1.89.
- 1190 [57] Geuzaine, C., Remacle, J.F., 2009. Gmsh: A 3-D finite element mesh
1191 generator with built-in pre- and post-processing facilities. *International*
1192 *Journal for Numerical Methods in Engineering* 79, 1309–1331. doi:10.
1193 1002/nme.2579.
- 1194 [58] Ghia, U., Ghia, K., Shin, C., 1982. High-Re solutions for incompressible
1195 flow using the Navier-Stokes equations and a multigrid method. *Journal*
1196 *of Computational Physics* 48, 387–411. doi:10.1016/0021-9991(82)
1197 90058-4.
- 1198 [59] Girault, V., Raviart, P.A., 2011. *Finite Element Methods for*
1199 *Navier-Stokes Equations*. Springer, Berlin, Heidelberg. doi:10.1007/
1200 978-3-642-61623-5.
- 1201 [60] Golo, G., Talasila, V., van der Schaft, A., Maschke, B., 2004. Hamilto-
1202 nian discretization of boundary control systems. *Automatica* 40, 757–
1203 771. doi:10.1016/j.automatica.2003.12.017.

- 1204 [61] Grmela, M., 2002. Lagrange hydrodynamics as extended Euler hydro-
 1205 dynamics: Hamiltonian and GENERIC structures. *Physics Letters A*
 1206 296, 97–104. doi:10.1016/S0375-9601(02)00190-1.
- 1207 [62] Grmela, M., Öttinger, H., 1997. Dynamics and thermodynamics of
 1208 complex fluids. I. Development of a general formalism. *Physical Review*
 1209 *E* 56, 6620–6632. doi:10.1103/PhysRevE.56.6620.
- 1210 [63] Gugercin, S., Polyuga, R.V., Beattie, C., van der Schaft,
 1211 A., 2012. Structure-preserving tangential interpolation for
 1212 model reduction of port-hamiltonian systems. *Automatica* 48,
 1213 1963–1974. URL: [https://www.sciencedirect.com/science/
 1214 article/pii/S0005109812002257](https://www.sciencedirect.com/science/article/pii/S0005109812002257), doi:[https://doi.org/10.1016/
 1215 j.automatica.2012.05.052](https://doi.org/10.1016/j.automatica.2012.05.052).
- 1216 [64] Haine, G., Matignon, D., 2021. Incompressible Navier-Stokes Equation
 1217 as port-Hamiltonian systems: velocity formulation versus vorticity for-
 1218 mulation. *IFAC-PapersOnLine* 54, 161–166. doi:10.1016/j.ifacol.
 1219 2021.11.072. 7th IFAC Workshop on Lagrangian and Hamiltonian
 1220 Methods for Nonlinear Control LHMNC 2021.
- 1221 [65] Haine, G., Matignon, D., Monteghetti, F., 2022a. Long-time behav-
 1222 ior of a coupled heat-wave system using a structure-preserving finite
 1223 element method. *Mathematical Reports* 24(74), 187–215.
- 1224 [66] Haine, G., Matignon, D., Monteghetti, F., 2022b. Structure-preserving
 1225 discretization of Maxwell’s equations as a port-Hamiltonian system.
 1226 *IFAC-PapersOnLine* 55, 424–429. doi:10.1016/j.ifacol.2022.11.
 1227 090. 25th International Symposium on Mathematical Theory of Net-
 1228 works and Systems MTNS 2022.
- 1229 [67] Haine, G., Matignon, D., Serhani, A., 2023. Numerical analysis of a
 1230 structure-preserving space-discretization for an anisotropic and hetero-
 1231 geneous boundary controlled N -dimensional wave equation as a port-
 1232 Hamiltonian system. *International Journal of Numerical Analysis &*
 1233 *Modeling* 20, 92–133. doi:10.4208/ijnam2023-1005.
- 1234 [68] Hamroun, B., Dimofte, A., Lefèvre, L., Mendes, E., 2010. Control
 1235 by Interconnection and Energy-Shaping Methods of Port Hamiltonian

- 1236 Models. Application to the Shallow Water Equations. *European Jour-*
1237 *nal of Control* 16, 545–563. doi:10.3166/ejc.16.545–563.
- 1238 [69] Hamroun, B., Lefèvre, L., Mendes, E., 2006. Port-based modelling for
1239 open channel irrigation systems. *Transactions on Fluid Mechanics* 1,
1240 995–1009.
- 1241 [70] Heidari, H., Zwart, H., 2019. Port-Hamiltonian modelling of nonlocal
1242 longitudinal vibrations in a viscoelastic nanorod. *Mathematical and*
1243 *Computer Modelling of Dynamical Systems* 25, 447–462. doi:10.1080/
1244 13873954.2019.1659374.
- 1245 [71] Hiemstra, R., Toshniwal, D., Huijsmans, R., Gerritsma, M., 2014. High
1246 order geometric methods with exact conservation properties. *Journal*
1247 *of Computational Physics* 257, 1444–1471. doi:10.1016/j.jcp.2013.
1248 09.027. physics-compatible numerical methods.
- 1249 [72] Jacob, B., Morris, K., 2022. On solvability of dissipative partial
1250 differential-algebraic equations. *IEEE Control Systems Letters* 6, 3188–
1251 3193. doi:10.1109/LCSYS.2022.3183479.
- 1252 [73] Jacob, B., Zwart, H.J., 2012. Linear port-Hamiltonian systems
1253 on infinite-dimensional spaces. Birkhäuser, Basel. doi:10.1007/
1254 978-3-0348-0399-1.
- 1255 [74] Jongschaap, R., 2001. The matrix model, a driven state vari-
1256 ables approach to non-equilibrium thermodynamics. *Journal of Non-*
1257 *Newtonian Fluid Mechanics* 96, 63–76. doi:https://doi.org/10.
1258 1016/S0377-0257(00)00136-1.
- 1259 [75] Jongschaap, R., Öttinger, H.C., 2004. The mathematical represen-
1260 tation of driven thermodynamic systems. *Journal of Non-Newtonian*
1261 *Fluid Mechanics* 120, 3–9. doi:https://doi.org/10.1016/j.jnnfm.
1262 2003.11.008. 3rd International workshop on Nonequilibrium Thermo-
1263 dynamics and Complex Fluids.
- 1264 [76] Kotyczka, P., 2019. Numerical Methods for Distributed Parameter
1265 Port-Hamiltonian Systems. TUM.University Press. doi:10.14459/
1266 2019md1510230.

- 1267 [77] Kotyczka, P., Maschke, B., Lefèvre, L., 2018. Weak form of Stokes–
1268 Dirac structures and geometric discretization of port-Hamiltonian sys-
1269 tems. *Journal of Computational Physics* 361, 442–476. doi:10.1016/
1270 j.jcp.2018.02.006.
- 1271 [78] Kraus, M., 2021. Metriplectic Integrators for Dissipative Fluids,
1272 in: *Geometric Science of Information*. Springer, Cham, pp. 292–301.
1273 doi:10.1007/978-3-030-80209-7_33.
- 1274 [79] Kunkel, P., Mehrmann, V., 2006. *Differential-Algebraic Equations:*
1275 *Analysis and Numerical Solution*. EMS Textbooks in Mathematics,
1276 European Mathematical Society, Zürich. doi:10.4171/017.
- 1277 [80] Kurula, M., Zwart, H., 2015. Linear wave systems on n-D spatial
1278 domains. *International Journal of Control* 88, 1063–1077. doi:10.1080/
1279 00207179.2014.993337.
- 1280 [81] Lagrée, P.Y., 2021. Equations de Saint Venant et application aux
1281 mouvements de fonds érodables. URL: [http://www.lmm.jussieu.fr/
1282 %7Elagree/COURS/MFEnv/MFEnv.pdf](http://www.lmm.jussieu.fr/%7Elagree/COURS/MFEnv/MFEnv.pdf). class notes.
- 1283 [82] Lamour, R., März, R., Tischendorf, C., 2013. *Abstract differential-*
1284 *algebraic equations*. Springer Berlin Heidelberg, Berlin, Heidelberg. pp.
1285 539–580. URL: https://doi.org/10.1007/978-3-642-27555-5_12,
1286 doi:10.1007/978-3-642-27555-5_12.
- 1287 [83] Le Gorrec, Y., Zwart, H., Maschke, B., 2005. Dirac Structures and
1288 Boundary Control Systems Associated with Skew-Symmetric Differen-
1289 tial Operators. *SIAM Journal on Control and Optimization* 44, 1864–
1290 1892. doi:10.1137/040611677.
- 1291 [84] Lequeurre, J., Munnier, A., 2020. Vorticity and Stream Function
1292 Formulations for the 2D Navier–Stokes Equations in a Bounded Do-
1293 main. *Journal of Mathematical Fluid Mechanics* 22, 15. doi:10.1007/
1294 s00021-019-0479-5.
- 1295 [85] Logg, A., Mardal, K.A., Wells, G., 2012. *Automated Solution of Dif-*
1296 *ferential Equations by the Finite Element Method*. Springer, Berlin,
1297 Heidelberg. doi:10.1007/978-3-642-23099-8.

- 1298 [86] Lohmayer, M., Kotyczka, P., Leyendecker, S., 2021. Exergetic port-
1299 Hamiltonian systems: modelling basics. *Mathematical and Computer*
1300 *Modelling of Dynamical Systems* 27, 489–521. doi:10.1080/13873954.
1301 2021.1979592.
- 1302 [87] Lopes, N., Hélie, T., 2016. Energy balanced model of a jet interacting
1303 with a brass player’s lip. *Acta Acustica united with Acustica* 102,
1304 141–154. doi:10.3813/AAA.918931.
- 1305 [88] Marche, F., 2007. Derivation of a new two-dimensional viscous shallow
1306 water model with varying topography, bottom friction and capillary
1307 effects. *European Journal of Mechanics B/Fluids* 26, 49–63. doi:10.
1308 1016/j.euromechflu.2006.04.007.
- 1309 [89] Maschke, B., van der Schaft, A., 2020. Linear Boundary Port
1310 Hamiltonian Systems defined on Lagrangian submanifolds. *IFAC-*
1311 *PapersOnLine* 53, 7734–7739. doi:10.1016/j.ifacol.2020.12.1526.
1312 21st IFAC World Congress 2020.
- 1313 [90] Mehrmann, V., Unger, B., 2023. Control of port-Hamiltonian
1314 differential-algebraic systems and applications. *Acta Numerica* 32, 395–
1315 515. doi:10.1017/S0962492922000083.
- 1316 [91] Mehrmann, V., van der Schaft, A., 2023. Differential–algebraic sys-
1317 tems with dissipative Hamiltonian structure. *Mathematics of Control,*
1318 *Signals, and Systems* 35, 541–584. doi:10.1007/s00498-023-00349-2.
- 1319 [92] Mehrmann, V., Zwart, H., 2024. Abstract dissipative Hamiltonian
1320 differential-algebraic equations are everywhere. *arXiv:2311.03091*.
- 1321 [93] Merker, J., Krüger, M., 2013. On a variational principle in thermo-
1322 dynamics. *Continuum Mechanics and Thermodynamics* 25, 779–793.
1323 doi:10.1007/s00161-012-0277-2.
- 1324 [94] Mohamed, M., Hirani, A., Samtaney, R., 2016. Discrete exterior calcu-
1325 lus discretization of incompressible Navier-Stokes equations over sur-
1326 face simplicial meshes. *Journal of Computational Physics* 312, 175–191.
1327 doi:10.1016/j.jcp.2016.02.028.

- 1328 [95] Mora, L.A., Le Gorrec, Y., Matignon, D., Ramirez, H., 2023. Irreversible port-Hamiltonian modelling of 3D compressible fluids. IFAC-PapersOnLine 56, 6394–6399. doi:10.1016/j.ifacol.2023.10.836.
1329
1330
1331 22nd IFAC World Congress.
- 1332 [96] Mora, L.A., Le Gorrec, Y., Matignon, D., Ramirez, H., Yuz, J.I., 2021. On port-Hamiltonian formulations of 3-dimensional compressible Newtonian fluids. Physics of Fluids 33, 117117. doi:10.1063/5.0067784.
1333
1334
- 1335 [97] Mora, L.A., Ramirez, H., Yuz, J.I., Le Gorrec, Y., Zañartu, M., 2020a. Energy-based fluid–structure model of the vocal folds. IMA Journal of Mathematical Control and Information 38, 466–492. doi:10.1093/imamci/dnaa031.
1336
1337
1338
- 1339 [98] Mora, L.A., Yann, L., Ramirez, H., Yuz, J., 2020b. Fluid-Structure Port-Hamiltonian Model for Incompressible Flows in Tubes with Time Varying Geometries. Mathematical and Computer Modelling of Dynamical Systems 26, 409–433. doi:10.1080/13873954.2020.1786841.
1340
1341
1342
- 1343 [99] Morandin, R., 2024. Modeling and Numerical Treatment of Port-Hamiltonian Descriptor Systems. Doctorate. Technische Universität Berlin. URL: <https://depositonce.tu-berlin.de/items/e9b3d954-dd50-48b0-85ce-9e9743d87479>.
1344
1345
1346
- 1347 [100] Morrison, P.J., 1984. Bracket formulation for irreversible classical fields. Physics Letters A 100, 423–427. doi:[https://doi.org/10.1016/0375-9601\(84\)90635-2](https://doi.org/10.1016/0375-9601(84)90635-2).
1348
1349
- 1350 [101] Morrison, P.J., 1998. Hamiltonian description of the ideal fluid. Reviews of Modern Physics 70, 467–521. doi:10.1103/RevModPhys.70.467.
1351
1352
- 1353 [102] Moses Badlyan, A., Maschke, B., Beattie, C.A., Mehrmann, V., 2018. Open Physical Systems: From GENERIC to Port-Hamiltonian Systems, in: Mathematical Theory of Networks and Systems (MTNS), Hong Kong, China. pp. 204–211.
1354
1355
1356
- 1357 [103] Moulla, R., Lefèvre, L., Maschke, B., 2012. Pseudo-spectral methods for the spatial symplectic reduction of open systems of conservation laws. Journal of Computational Physics 231, 1272–1292. doi:10.1016/j.jcp.2011.10.008.
1358
1359
1360

- 1361 [104] Mrugala, R., Nulton, J., Schon, J., Salamon, P., 1991. Contact struc-
 1362 ture in thermodynamic theory. *Reports in Mathematical Physics* 29,
 1363 109–121. doi:10.1016/0034-4877(91)90017-H.
- 1364 [105] Ngoc Minh Trang Vu, L.L., Maschke, B., 2016. A structured control
 1365 model for the thermo-magneto-hydrodynamics of plasmas in tokamaks.
 1366 *Mathematical and Computer Modelling of Dynamical Systems* 22, 181–
 1367 206. doi:10.1080/13873954.2016.1154874.
- 1368 [106] Olver, P.J., 1993. Applications of Lie Groups to Differential Equa-
 1369 tions. volume 107 of *Graduate Texts in Mathematics*. 2nd ed., Springer-
 1370 Verlag, New York. doi:10.1007/978-1-4684-0274-2.
- 1371 [107] Öttinger, H., Grmela, M., 1997. Dynamics and thermodynamics of
 1372 complex fluids. II. Illustrations of a general formalism. *Physical Review*
 1373 *E* 56, 6633–6655. doi:10.1103/PhysRevE.56.6633.
- 1374 [108] Pasumathy, R., Ambati, V., van der Schaft, A., 2008. Port-
 1375 Hamiltonian formulation of shallow water equations with Coriolis force
 1376 and topography, in: *Mathematical Theory of Networks and Systems*
 1377 (MTNS), Blacksburg, VA, USA.
- 1378 [109] Pasumathy, R., Ambati, V.R., van der Schaft, A.J., 2012. Port-
 1379 Hamiltonian discretization for open channel flows. *Systems & Control*
 1380 *Letters* 61, 950–958. doi:10.1016/j.sysconle.2012.05.003.
- 1381 [110] Payen, G., Matignon, D., Haine, G., 2020. Modelling and structure-
 1382 preserving discretization of Maxwell’s equations as port-Hamiltonian
 1383 system. *IFAC-PapersOnLine* 53, 7581–7586. doi:10.1016/j.ifacol.
 1384 2020.12.1355. 21st IFAC World Congress.
- 1385 [111] Philipp, F., Reis, T., Schaller, M., 2023. Infinite-dimensional port-
 1386 Hamiltonian systems – a system node approach. *arXiv:2302.05168*.
- 1387 [112] Ramirez, H., Le Gorrec, Y., 2016. An irreversible port-Hamiltonian
 1388 formulation of distributed diffusion processes. *IFAC-PapersOnLine*
 1389 49, 46–51. doi:10.1016/j.ifacol.2016.10.752. 2th IFAC Workshop
 1390 on Thermodynamic Foundations for a Mathematical Systems Theory
 1391 TFMST 2016.

- 1392 [113] Ramirez, H., Le Gorrec, Y., 2022. An overview on irreversible port-
1393 Hamiltonian systems. *Entropy* 24, 1478. doi:10.3390/e24101478.
- 1394 [114] Ramirez, H., Le Gorrec, Y., Maschke, B., 2022. Boundary controlled
1395 irreversible port-Hamiltonian systems. *Chemical Engineering Science*
1396 248, 117107. doi:10.1016/j.ces.2021.117107.
- 1397 [115] Ramirez, H., Maschke, B., Sbarbaro, D., 2013. Irreversible port-
1398 Hamiltonian systems: A general formulation of irreversible processes
1399 with application to the CSTR. *Chemical Engineering Science* 89, 223–
1400 234. doi:10.1016/j.ces.2012.12.002.
- 1401 [116] Rashad, R., Califano, F., van der Schaft, A.J., Stramigioli, S., 2020.
1402 Twenty years of distributed port-Hamiltonian systems: a literature
1403 review. *IMA Journal of Mathematical Control and Information* 37,
1404 1400–1422. doi:10.1093/imamci/dnaa018.
- 1405 [117] Rashad, R., Califano, F., Schuller, F.P., Stramigioli, S., 2021a. Port-
1406 Hamiltonian modeling of ideal fluid flow: Part I. Foundations and ki-
1407 netic energy. *Journal of Geometry and Physics* 164, 104201. doi:10.
1408 1016/j.geomphys.2021.104201.
- 1409 [118] Rashad, R., Califano, F., Schuller, F.P., Stramigioli, S., 2021b. Port-
1410 Hamiltonian modeling of ideal fluid flow: Part II. Compressible and
1411 incompressible flow. *Journal of Geometry and Physics* 164, 104199.
1412 doi:10.1016/j.geomphys.2021.104199.
- 1413 [119] Reis, T., Schaller, M., 2023. Port-Hamiltonian formulation of Oseen
1414 flows. [arXiv:2305.09618](https://arxiv.org/abs/2305.09618).
- 1415 [120] Rettberg, J., Wittwar, D., Buchfink, P., Brauchler, A., Ziegler, P.,
1416 Fehr, J., Haasdonk, B., 2023. Port-Hamiltonian fluid–structure inter-
1417 action modelling and structure-preserving model order reduction of a
1418 classical guitar. *Mathematical and Computer Modelling of Dynamical*
1419 *Systems* 29, 116–148. doi:10.1080/13873954.2023.2173238.
- 1420 [121] van der Schaft, A., 2021. Classical thermodynamics revisited: A sys-
1421 tems and control perspective. *IEEE Control Systems Magazine* 41,
1422 32–60.

- 1423 [122] van der Schaft, A., Maschke, B., 2018a. Generalized port-Hamiltonian
1424 DAE systems. *Systems & Control Letters* 121, 31–37. doi:10.1016/j.
1425 sysconle.2018.09.008.
- 1426 [123] van der Schaft, A., Maschke, B., 2018b. Geometry of Thermodynamic
1427 Processes. *Entropy* 20, 925. doi:10.3390/e20120925.
- 1428 [124] van der Schaft, A.J., 2013. Port-Hamiltonian Differential-Algebraic
1429 Systems. Springer, Berlin, Heidelberg. pp. 173–226. doi:10.1007/
1430 978-3-642-34928-7\5.
- 1431 [125] van der Schaft, A.J., Jeltsema, D., 2014. Port-Hamiltonian Systems
1432 Theory: An Introductory Overview. *Foundations and Trends® in*
1433 *Systems and Control* 1, 173–378. doi:10.1561/26000000002.
- 1434 [126] van der Schaft, A.J., Maschke, B.M., 2002. Hamiltonian formulation
1435 of distributed-parameter systems with boundary energy flow. *Journal*
1436 *of Geometry and Physics* 42, 166–194. doi:10.1016/S0393-0440(01)
1437 00083-3.
- 1438 [127] Schiebl, M., Betsch, P., 2021. Structure-preserving space-time dis-
1439 cretization of large-strain thermo-viscoelasticity in the framework of
1440 GENERIC. *International Journal for Numerical Methods in Engineer-*
1441 *ing* 122, 3448–3488. doi:https://doi.org/10.1002/nme.6670.
- 1442 [128] Serhani, A., Matignon, D., Haine, G., 2019a. A partitioned finite el-
1443 element method for the structure-preserving discretization of damped
1444 infinite-dimensional port-Hamiltonian systems with boundary control,
1445 in: *Geometric Science of Information*. Springer, Cham, pp. 549–558.
1446 doi:10.1007/978-3-030-26980-7\57.
- 1447 [129] Serhani, A., Matignon, D., Haine, G., 2019b. Anisotropic hetero-
1448 geneous n -D heat equation with boundary control and observation:
1449 II. Structure-preserving discretization. *IFAC-PapersOnLine* 52, 57–62.
1450 doi:10.1016/j.ifacol.2019.07.009. 3rd IFAC Workshop on Ther-
1451 modynamic Foundations for a Mathematical Systems Theory (TFMST
1452 2019).
- 1453 [130] Serhani, A., Matignon, D., Haine, G., 2019c. Partitioned Finite Ele-
1454 ment Method for port-Hamiltonian systems with Boundary Damping:

- 1455 Anisotropic Heterogeneous 2D wave equations. IFAC-PapersOnLine
1456 52, 96–101. doi:10.1016/j.ifacol.2019.08.017. 3rd IFAC Work-
1457 shop on Control of Systems Governed by Partial Differential Equations
1458 CPDE 2019.
- 1459 [131] Seslija, M., van der Schaft, A., Scherpen, J.M., 2012. Discrete
1460 exterior geometry approach to structure-preserving discretization of
1461 distributed-parameter port-Hamiltonian systems. *Journal of Geometry
1462 and Physics* 62, 1509–1531. doi:10.1016/j.geomphys.2012.02.006.
- 1463 [132] Skrepek, N., 2021. Well-posedness of linear first order port-Hamiltonian
1464 systems on multidimensional spatial domains. *Evolution Equations and
1465 Control Theory* 10, 965–1006. doi:10.3934/eect.2020098.
- 1466 [133] Temam, R., 2001. *Navier-Stokes Equations: Theory and Numerical
1467 Analysis*. Revised edition ed., American Mathematical Society.
- 1468 [134] Thuburn, J., Cotter, C.J., 2015. A primal-dual mimetic finite element
1469 scheme for the rotating shallow water equations on polygonal spherical
1470 meshes. *Journal of Computational Physics* 290, 274–297. doi:10.1016/
1471 j.jcp.2015.02.045.
- 1472 [135] Trenchant, V., Ramirez, H., Le Gorrec, Y., Kotyczka, P., 2018. Finite
1473 differences on staggered grids preserving the port-hamiltonian structure
1474 with application to an acoustic duct. *Journal of Computational Physics*
1475 373, 673–697. doi:10.1016/j.jcp.2018.06.051.
- 1476 [136] van der Schaft, A., Maschke, B., 1994. On the Hamiltonian formula-
1477 tion of nonholonomic mechanical systems. *Reports on Mathematical
1478 Physics* 34, 225–233.
- 1479 [137] van der Schaft, A., Mehrmann, V., 2023. Linear port-Hamiltonian DAE
1480 systems revisited. *Systems & Control Letters* 177, 105564. doi:10.
1481 1016/j.sysconle.2023.105564.
- 1482 [138] Villegas, J., Le Gorrec, Y., Zwart, H., Maschke, B., 2006. Boundary
1483 control for a class of dissipative differential operators including diffusion
1484 systems, in: *Mathematical Theory of Networks and Systems (MTNS)*,
1485 Kyoto, Japan Kyoto, Japan. pp. 24–28.

- 1486 [139] Vu, N.M.T., Lefèvre, L., Nouailletas, R., Brémond, S., 2017. Sym-
1487 plectic spatial integration schemes for systems of balance equations.
1488 Journal of Process Control 51, 1–17. doi:10.1016/j.jprocont.2016.
1489 12.005.
- 1490 [140] Vu, N.M.T., Lefèvre, L., Maschke, B., 2019. Geometric spatial reduc-
1491 tion for port-Hamiltonian systems. Systems & Control Letters 125,
1492 1–8. doi:10.1016/j.sysconle.2019.01.002.
- 1493 [141] Warsewa, A., Böhm, M., Sawodny, O., Tarín, C., 2021. A port-
1494 Hamiltonian approach to modeling the structural dynamics of com-
1495 plex systems. Applied Mathematical Modelling 89, 1528–1546. doi:10.
1496 1016/j.apm.2020.07.038.
- 1497 [142] Zhang, Y., Palha, A., Gerritsma, M., Rebholz, L.G., 2022. A mass-
1498 , kinetic energy- and helicity-conserving mimetic dual-field discretiza-
1499 tion for three-dimensional incompressible Navier-Stokes equations, part
1500 I: Periodic domains. Journal of Computational Physics 451, 110868.
1501 doi:10.1016/j.jcp.2021.110868.
- 1502 [143] Öttinger, H.C., 2018. Generic integrators: Structure preserving time
1503 integration for thermodynamic systems. Journal of Non-Equilibrium
1504 Thermodynamics 43, 89–100. doi:doi:10.1515/jnet-2017-0034.